LBL-2874
c. 2

ELECTRON MICROSCOPY AT REDUCED LEVELS OF IRRADIATION

DONNER LABORATORY

Ivy Ai-Ming Kuo
(Ph. D. thesis)

May 1975

Prepared for the U. S. Energy Research and Development Administration under Contract W-7405-ENG-48

TWO-WEEK LOAN COPY

This is a Library Circulating Copy which may be borrowed for two weeks. For a personal retention copy, call Tech. Info. Division,

LAWRENCE BERKELEY LABORATORY • UNIVERSITY OF CALIFORNIA • BERKELEY

LBL-2874
c. 2

DISCLAIMER

This document was prepared as an account of work sponsored by the United States Government. While this document is believed to contain correct information, neither the United States Government nor any agency thereof, nor the Regents of the University of California, nor any of their employees, makes any warranty, express or implied, or assumes any legal responsibility for the accuracy, completeness, or usefulness of any information, apparatus, product, or process disclosed, or represents that its use would not infringe privately owned rights. Reference herein to any specific commercial product, process, or service by its trade name, trademark, manufacturer, or otherwise, does not necessarily constitute or imply its endorsement, recommendation, or favoring by the United States Government or any agency thereof, or the Regents of the University of California. The views and opinions of authors expressed herein do not necessarily state or reflect those of the United States Government or any agency thereof or the Regents of the University of California.

ELECTRON MICROSCOPY AT REDUCED LEVELS OF IRRADIATION

ABSTRACT

Ivy Ai-Ming Kuo

Specimen damage by electron radiation is one of the factors that limits high resolution electron microscopy of biological specimens. The purpose of the work in this thesis is to develop a method to record images of periodic objects at a reduced electron exposure in order to preserve high resolution structural detail. The resulting image would tend to be a statistically noisy one, as the electron exposure is reduced to lower and lower values. Reconstruction of a statistically defined image from such data is possible by spatial averaging of the electron signals from a large number of identical unit cells. We choose to refer to this general approach for reducing the effects of radiation damage as the Statistically Noisy, Averaged Picture (SNAP-shot) method.

Kodak Nuclear Track Plates, type NTB2, processed by infectious development were found to be a highly sensitive recording medium. Images have been recorded with exposures as low as 10^{-3} electron/μm^2. Results that have been obtained with an image intensifier, and a few of the other commercially available fast emulsions are also discussed.

TABLE OF CONTENTS

	Page
ABSTRACT	ii
CHAPTER 1 INTRODUCTION	1
1.1 Effects of Electron Radiation on Biological Specimens	2
1.2 Attempts to Minimize Radiation Damage	4
1.3 The SNAP-shot Method	7
CHAPTER 2 THEORY	
2.1 The Minimum Beam Exposure Technique	9
2.2 Critical Exposure	9
2.3 The Rose Equation	10
2.4 The SNAP-shot Method	12
2.5 The Recording Device for a Statistically Noisy Image	13
2.6 Improvement in Resolution by the SNAP-shot Method	13
2.7 Extending the SNAP-shot Method to Non-periodic Image Features	15
CHAPTER 3 PRELIMINARY STUDIES OF THE SNAP-SHOT METHOD	
3.1 Numerical Simulation of a SNAP-shot	17
3.2 Image Intensifier	20
3.3 Computer Processing of Image Data	22
3.4 Results with the Image Intensifier	26
3.5 Evaluation of the Image Intensifier as a SNAP-shot Recorder	27
CHAPTER 4 PHOTOGRAPHIC EMULSIONS	29
4.1 Determination of Grain Size and Fog Level	29

4.2 Statistically Noisy Images on Medical X-ray Film 32

4.3 Removal of Fog Grains in Medical X-ray Film 32

4.4 Infectious Development of Medical X-ray Film 34

4.5 The Use of Phosphorescent Screens to Amplify the Electron Signals 36

CHAPTER 5 KODAK NUCLEAR TRACK EMULSION (TYPE NTB2) 41

5.1 Electron Microscopy 46

5.2 Optical Diffraction and Microdensitometry 47

5.3 Signal Amplification and Noise Suppression on the NTB2 Emulsion 48

5.4 Grating Resolution of NTB2 Emulsion 48

5.5 Present Status of Experimental Results with NTB2 49

5.6 Best Attainable Resolution of the SNAP-shot Method Using NTB2 57

5.7 Contrast of Infectiously Developed NTB2 61

5.8 Evaluation of the NTB2-Infectious Development Approach 63

5.9 Discussion 64

APPENDIX Computer Program Listings 69

BIBLIOGRAPHY 117

ACKNOWLEDGMENTS 122

CHAPTER 1

INTRODUCTION

Biological electron microscopy has been very useful in the study of the cellular structures that are too small to be resolved by the light microscope. Instrumental development of the electron microscope in recent years has greatly improved the resolving power of the electron microscope, such that lattice resolution of 1-2 Å is possible (25,56). In addition, the transfer function theory of the electron microscope is now better understood (49), and the phase distortion caused by misfocusing, spherical aberration, and astimatism can be corrected to high resolutions by the use of numerical image reconstruction techniques (14,15). Furthermore, three dimensional image reconstruction of an object is possible from images of the same object taken at different tilt angles (8,9). It seems, therefore, that the electron microscope can be a very powerful tool in the study of structure at the molecular level.

Contrary to what is expected on the basis of the high instrumental performance, at present only cellular structures larger than ∿40 Å can be resolved in the electron microscope. The reasons for this are many. One of the problems is that of specimen preparation. Techniques such as dehydration, embedding, fixation and staining (18), are necessary in order to increase the specimen contrast and to

render the specimen more resistant to the high vacuum of the microscope column. A necessary consequence of these specimen manipulations appears to be that only structures larger than 40 Å remain intact.

1.1 Effects of electron radiation on biological specimens

One important limitation to high resolution electron microscopy of biological specimens is that of electron radiation damage. This subject has been reviewed extensively by Stenn and Bahr (42). In the electron microscope, a small number of the electrons passing through the specimen will be inelastically scattered. As energy is transferred from the electrons to the specimen, excited, ionized and radical species are formed. These chemically active species will tend to combine with other charged ions or with electrons to reach a more stable state. The molecular changes that follow can be generalized into the following catagories. (1) Bond dissociation and loss of small side groups, resulting in mass loss (2,33,47) and fragmentation of larger molecules into smaller ones. (2) Formation of new bonds: cross-linking between neighbouring molecules or with a contiguous portion of the same molecule (7). (3) Changing of bond type: on losing hydrogen, an organic molecule acquires double and triple bonds (42).

Structural changes are well demonstrated in infra-red spectra taken of irradiated samples. The spectral patterns

show a progressive decrease in absorption intensity and a decrease in pattern complexity as the electron exposure increases (2,33). In addition, the progressive fading of electron diffraction patterns of organic crystals (16,33) indicates structural disorder.

The secondary and tertiary structures of organic molecules are dependent on weak bonds (e.g., hydrogen bonds, hydrophobic interactions, and van der Waals bonds), and these bonds can be disrupted by the absorption of a small amount of energy (0.1 - 1 ev) (42). It is therefore important to determine what is the lowest electron exposure that causes complete structural damage to the irradiated specimen. A variety of methods have been used to assess the extent of specimen damage. Fading and changes of electron diffraction patterns of crystalline specimens indicate loss of crystalline order and structural alterations (16,33). Structural changes can also be studied by observing the changes in the absorption spectra (infrared, visible, and ultraviolet) of the irradiated specimen (33, 42). In addition, mass loss of the specimen can be measured by directly weighing the material or by autoradiography (10,33,47). From these studies, it was found that for each type of molecule, there is a maximal level of electron exposure that can be tolerated. After the exposure reaches this value, the accumulation of structural

changes in the specimen is such that further observation probably will provide no meaningful information concerning the original structure. In the rest of our discussion, we will refer to this level of exposure as the critical exposure[1].

1.2 Attempts to minimize radiation damage

In view of the disorder of molecular arrangement resulting from electron exposure, it is apparent that the development of methods to reduce radiation damage is essential. This might be accomplished either by minimization of the amount of exposure to the incident radiation, or by making the specimen more resistant to the effects of the inelastically scattered electrons. A few of the methods used to minimize the effects of radiation damage are briefly discussed in the rest of this section.

High voltage electron microscopy is considered as a possible way to increase the value of the critical exposure. It is known that the loss of energy from the electron beam is proportional to the inverse square of the electron velocity (5). Therefore it is possible that the high velocity electrons in the high voltage microscope would cause less damage to the specimen. Experimental

---

[1]At the plane of the specimen in the electron microscope, the critical exposure will be expressed in units of coulomb/cm^2, or electron/$Å^2$. At the image plane, it will be expressed in units of electron/μm^2.

studies on the voltage dependence of critical exposure have established that between the voltages of 80 Kev and 1 Mev, the critical exposure increases by a factor of 2 to 3 (17).

Theoretical calculation of both bright-field and dark-field image intensities of single atoms reveals an additional advantage in going to higher voltages (34,37,57). Due to the increase in depth of field and reduction in chromatic aberration, the image contrast of individual atoms increases at energies above 1 Mev. Because of the higher contrast, much lower electron exposures could be used to resolve the atomic positions. However, in order to achieve single atom imaging, it is necessary to use a high voltage microscope with 1 Å resolving power. At present, no existing high voltage electron microscope can operate at this resolution; the principal difficulties being that of achieving good electrical and mechanical stability at energies as high as 1 Mev.

Another possible method to use for decreasing the radiation damage effect is that of very low specimen temperature. Electron diffraction studies of paraffin and tetracene, both at 300°K and 4°K, have shown that the critical exposures at 4°K are larger by a factor of 2 or more (38). At the lower temperature, it is possible that the molecular fragments resulting from bond dissociation are less likely to diffuse from their original positions.

Consequently, the structures of the organic crystals can be maintained up to higher levels of exposure. The effect of increased specimen resistance to the electron beam at low temperature was also demonstrated in the case of hydrated specimens. The critical exposures of unstained, hydrated catalase crystals have been determined by electron diffraction studies, both at room temperature and at liquid nitrogen temperature (28,46). The critical exposure of the frozen hydrated catalase was found to be larger by a factor of 10. This significant improvement in the critical exposure is still not large enough to enable direct imaging of molecular structures.

In addition to the methods mentioned above which have general applications, it is possible that special methods may be found to be of help in specific cases. Salih (36) reported increased resistance to damage by as much as a factor of 4 to 5, when a 500 Å thick coronene crystal was sandwiched between thin films of gold or aluminum. However, this observation has not yet been confirmed by other investigators. The electron diffraction pattern of catalase stained with uranyl/aluminum (1/1) formate, was found to have increased fading time (50). This effect was attributed to the experimentally documented fact that this stain mixture forms inorganic micro-crystals at a slower rate than does the normal uranyl acetate stain.

1.3 The SNAP-shot Method

As a consequence of the high sensitivity of organic molecules to electron radiation, the structural information that possibly can be obtained from electron-specimen interactions is severly limited. The methods described above aim mainly at increasing the critical exposure. But even a several fold increase in the critical exposure is still not sufficient for imaging high resolution detail of low contrast. In the work reported here, we investigated the feasibility of obtaining high resolution image data of periodic biological specimens if the images were recorded at an exposure not exceeding the critical exposure for the specimen.

A method of recording images of periodic objects at a reduced electron exposure has been developed. The resulting image must tend to be a statistically noisy one, as the electron exposure is reduced to lower and lower values. Construction of statistically defined image intensities from such data is possible by spatial averaging of the electron signals from a large number of identical unit cells. We choose to refer to this general approach for reducing the effects of radiation damage as the Statistically Noisy, Averaged Picture (SNAP-shot) method. A mathematical interpretation of the SNAP-shot method is presented in chapter 2.

The possibility of reconstruction of a statistically

defined image from a periodic, noisy image was first confirmed by a numerical simulation study. The procedure was also tested with data collected by the use of an image intensifier.

Owing to the low electron detection efficiency of the image intensifier (discussed in section 3.5), a large proportion of the electrons reaching the image plane were not detected. Photographic emulsions, being highly efficient in electron detection (52), were also experimented with for recording statistically noisy images. Latent images were amplified chemically by a procedure of infectious development (41). Kodak Nuclear Track Plates, type NTB2, when developed infectiously, were found to be best suited for our purpose. With exposures as low as 10^{-3} electrons/μm^2, Nuclear Track Plate can be developed to an optical density as high as 3 (figure 8), while the fog level remains insignificant (optical density less than 0.1).

CHAPTER 2

THEORY

2.1 The Minimum Beam Exposure Technique

Williams and Fisher (55) demonstrated that by limiting the total number of electrons to the amount necessary to form an image on a conventional electron image plate, there was a marked improvement in image resolution for negatively stained Tobacco Mosaic Viruses. The 23 Å periodicity of the virus, which had previously never been recorded, was clearly visible. However, the minimum beam method requires an exposure much higher than the critical exposure for most organic compounds (section 2.2). The high exposure is necessary to give an observable image of optical density $\sim$1 on the photographic plate. It is for this reason that recording of higher resolution detail will not be possible with this method alone.

2.2 Critical Exposure

The susceptibility of biological specimens to radiation damage demands that imaging must always be carried out with exposures not exceeding the critical value (N_{cr}) for damage. The critical exposures for some biological specimens have been established (16,33), and they generally are not smaller than the value of 10^{-3} coulomb/cm^2. Aromatic organic compounds are more resistant to radiation damage, and the critical exposure can approach 10^2 coulomb/cm^2

(60,000 electrons/Å^2) for some exceptional aromatic molecules.

The problem of image recording at the N_{cr} or less is two-fold: (1) At this level of exposure there is insufficient darkening of the photographic plate to yield an image observable to the eye or detectable by a scanning microdensitometer, except at very low magnification. (2) High resolution is not possible because of the small signal to noise ratio. The SNAP-shot method proposed here is one way to increase the signal to noise ratio for periodic objects.

2.3 The Rose Equation

The relationship between the attainable resolution (d) for a specified contrast (C) and the number of incident electrons per unit area (n) is given by the Rose equation (22):

$$Cd \geq \frac{5}{(n)^{\frac{1}{2}}} \qquad (2.1)$$

The contrast (C) is defined as the difference in intensity between two image points, separated by the distance d, divided by the average intensity of the two points. The value of 5 in the numerator was determined by visual perception experiments. These experiments have shown that the image contrast must exceed the fluctuation in the number of electrons $(1/(nd^2)^{\frac{1}{2}})$ by a factor of 5, for the image detail to be seen. For a given value of C, the image is said to be statistically defined at a resolution of d, if n satis-

fies the equation; otherwise, it is statistically noisy. Contrast values for biological molecules are usually very low; when the contrast is improved by staining, for resolutions above 25 Å, the contrast in any one Fourier component of the image is usually not better than 1% (7). In order to resolve 10 Å, we can see that from the Rose equation that n is calculated to be at least 2500 electrons/Å^2. For some aromatic compounds, the critical exposure (60,000 electrons/Å^2) far exceeds this value, and 10 Å resolution or better should be possible. This has been demonstrated experimentally in the case of Cu-hexadecachlorophthalocyanine (51). For saturated bond organic molecules, the value of 2500 electrons/Å^2 exceeds the critical exposure by a factor of 4000 or more, and 10 Å resolution should be impossible to attain.

Substituting n by the critical exposure N_{cr}, equation (2.1) can be adapted to the case of electron microscopy (17):

$$d \geq \frac{5}{C(fN_{cr})^{\frac{1}{2}}} \qquad (2.2)$$

where f, the net utilization factor, is the fraction of the critical exposure at the specimen which actually contributes to the formation of the image at the photographic plate. This factor takes into account the loss of electrons in various imaging modes, and the detection efficiency of the image recorder. Equation (2.2) reveals that an improve-

ment in the attainable resolution is possible by increasing the value for C, f and N_{cr}. Since d has an inverse square root dependence on f and N_{cr}, the effect of increased contrast is largest. The various methods outlined in chapter 1 have achieved but a modest increase in N_{cr}; thus, only a small improvement in d is expected from their use.

2.4 The SNAP-shot Method

In the electron microscope, if the electron irradiation is not to exceed the critical exposure, the recorded image (assuming even that we have a device capable of detecting single electrons), would be a statistically noisy one. However, if the specimen is periodic, and the unit cell dimension is known, then it is possible to spatially average the noisy image to yield a statistically defined image of a unit cell (16,27). If the noisy image is composed of R unit cells formed on the recorder, then after spatial averaging the number of electrons per resolution element is increased by a factor of R. In equation (2.1), n will be substituted by RxN_{cr}, instead of N_{cr}; where R is the number of repeating unit cells in the recorded image. The Rose equation then becomes

$$d_s \geq \frac{5}{C(fRN_{cr})^{\frac{1}{2}}} \qquad (2.3)$$

where d_s is the attainable resolution for the SNAP-shot method.

The periodicity of the object can be determined from the Fourier transform of the image (chapter 3.1, 3.3), and a Markham-type real space superposition procedure (27) can be subsequently applied to get the statistically defined image. Alternatively, a delta-function filtering performed on the reciprocal lattice will yield the same spatially averaged image. The mathematical justification for the latter approach has been elucidated by Aebi *et al*. (1).

2.5 The recording device for a statistically noisy image

The SNAP-shot method cannot be realized without a recording device that fulfills the following three requirements.

(1) It is capable of amplification of single electron events.

(2) It has a high value of Detective Quantum Efficiency (DQE), where $DQE = \frac{(\text{signal/noise})^2 \text{ of recorded image}}{(\text{signal/noise})^2 \text{ of electron beam}}$.

When DQE is equal to 1, the fluctuations in the image are caused only by the statistical fluctuations of the electron beam.

(3) It has a large detector area for data collection.

2.6 Improvement in resolution by the SNAP-shot method

Assuming the dimension of the image area is AxB, and that of the unit cell is axb; then the maximum number of repeating units, R, can be expressed as

$$R = \frac{A \cdot B}{(M \cdot a)(M \cdot b)} = \frac{r}{M^2} ,$$

where $r = (A \cdot B)/(a \cdot b)$, the ratio of image area to the unit cell area; M is the magnification.

Equation (2.3) becomes:

$$d_s \geq \frac{M}{r^{\frac{1}{2}}} \cdot \frac{5}{C(fN_{cr})^{\frac{1}{2}}} \qquad (2.4)$$

$$= \frac{M}{r^{\frac{1}{2}}} \cdot d \qquad (2.5)$$

where d is the attainable resolution before spatial averaging. d_s cannot be made arbitrarily small by decreasing M, because of the finite size of the minimum picture element (p) that can be resolved on the recording medium. Thus the additional condition

$$Md_s \geq p \qquad (2.6)$$

must also be satisfied. Equation (2.5) can be written with a trivial change as

$$d_s^2 \geq \frac{Md_s}{r^{\frac{1}{2}}} \cdot d.$$

Then, substituting Md_s by p, it becomes

$$d_s^2 \geq \frac{p}{r^{\frac{1}{2}}} \cdot d$$

$$\text{or} \quad d_s \geq \frac{p^{\frac{1}{2}}}{r^{\frac{1}{4}}} d^{\frac{1}{2}} \qquad (2.7)$$

Equation (2.7) expresses the best possible improvement in resolution, when the optimal choice of magnification is

used.

The following is a calculation using typical values to illustrate the improvement in resolution. Assuming $p = 10^6$ Å, AxB = (9 cm x 9 cm) = 81×10^{16} Å^2, and axb = (100 Å x 100 Å), equation (2.7) becomes

$$d_s \geq \frac{d^{\frac{1}{2}}}{3} .$$

d_s has a square root dependence on d, and is expressed in units of Ångstrom. d/d_s can be used as a measure of improvement in resolution. Several values for d, d_s and d/d_s are listed in table 1. The improvement in resolution becomes less significant as d becomes smaller.

2.7 Extending the SNAP-shot method to non-periodic image features

Extension of the method to non-periodic objects is theoretically possible. Frank (13) has proposed a procedure of matched filtering, by which noisy images of objects that have identical structure can be recognized and located. A cross-correlation procedure can then be used to place the noisy images in correct register, and the defined image is constructed from the superposition of the required number of noisy images.

TABLE 1

Predicted Improvement in Resolution by the SNAP-shot Method*

Attainable Resolution at Critical Exposure $d(\mathring{A})$	Attainable Resolution of SNAP-shot Method $d_s(\mathring{A})$	Improvement by SNAP-shot Method d / d_s
100	3.3	30
25	1.6	15
9	1.0	9
4	0.7	5.7
1	0.3	3.3

*Values of d are initial, arbitrary values, and values for d_s are the corresponding results for optimal magnification with the assumption of typical specimen parameters and detector resolution as listed in the text. Altering these parameters will of course give new values for d_s.

CHAPTER 3

PRELIMINARY STUDIES OF THE SNAP-SHOT METHOD

3.1 Numerical Simulation of a SNAP-shot

The feasibility of the SNAP-shot method was first tested by a numerical simulation with the computer. The specimen was assumed to have a checker-board pattern (figure 1) which was represented in the computer by a square array of 128 x 128 points. Incident electrons were simulated by generating numbers of value 1, which were added to elements of the array in a random fashion, thereby generating the resulting noisy image. Initially, all 128 x 128 elements were set to zero. The stochastic distribution of events was arranged such that the probability of an event falling on the dark area was twice that of an event falling on the light area. Figure 2a is the resulting statistically noisy image of the checker-board pattern, which has been displayed through a 3-D perspective, Calcomp plotting routine. From the power spectrum of the noisy image (figure 2b), the periodicity of the object was determined by measuring the vectors in the reciprocal lattice. Spatial averaging was done as follows: A real space lattice was superimposed on the noisy image, and the coordinates of each single-electron event were determined within its unit cell. Next all single-electron events were referred to their appropriate positions in one given unit cell. The pattern of

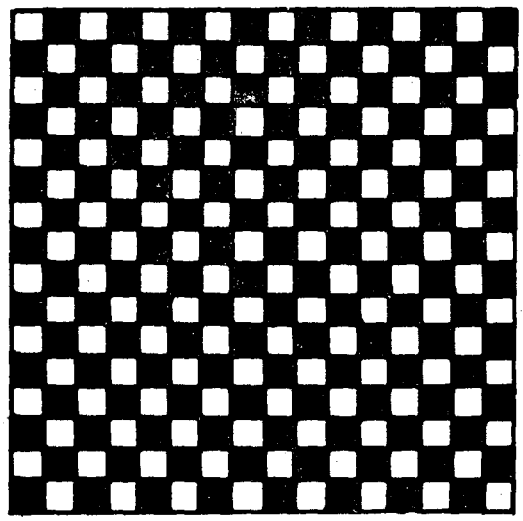

Fig. 1 A checkerboard pattern. Dark area has a value of 2, and light area has a value of 1. This pattern is represented in the computer program by a 128 x 128 array.

XBL 753-4791

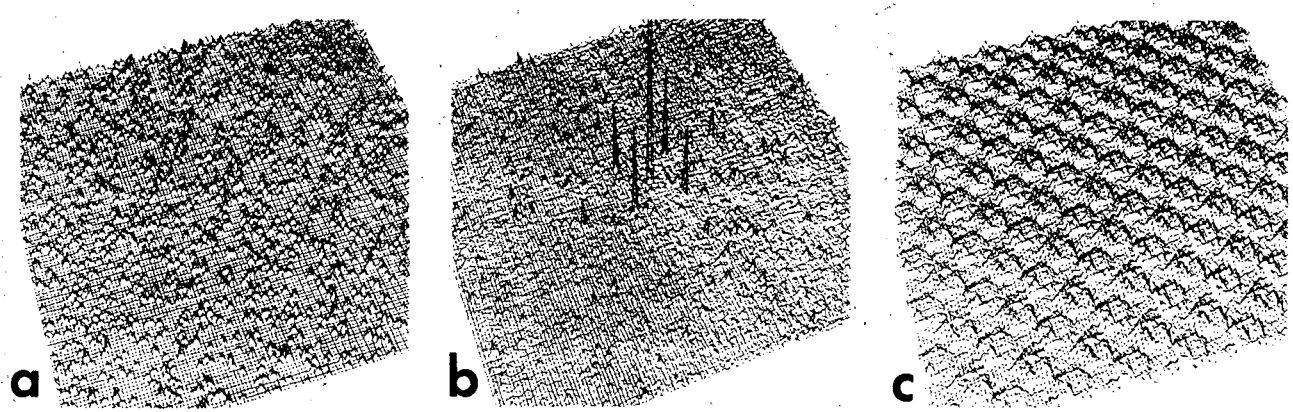

XBB 751-55

Fig. 2. Computer simulation of SNAP-shot method.
a. A 3-D perspective, Calcomp plot of a statistically noisy image of the pattern in fig. 1; b. the power spectrum of the statistically noisy image; c. the spatially averaged image.

the statistically determined unit cell was then repeated over the entire 128 x 128 array (figure 2c).

3.2 Image Intensifier

Application of the SNAP-shot method to experimental data was first attempted on data recorded by a commercially available image intensifier. The camera is of the Secondary Electron Conduction (SEC) vidicon type (Quantex Corp. Mountain View, Calif.). The camera is preceded by a one stage, electrostatic intensifier tube with a measured photon gain of 40. The intensifier looks at a scintillator screen, and fiber optics coupling is used throughout.

The amplified images were stored on a video disc recorder (VAS Ltd., Sunnyvale, Calif.) in consecutive frames. A selected frame was then continuously replayed to allow a slow-scan converter to sample and digitize the recorded image. The digitized data were stored on a magnetic tape to be used as input to a spatial averaging computer program. The flow diagram for data acquisition is shown in Fig. 3.

In order to determine the detection efficiency of the image intensifier an arbitrarily chosen video line was displayed on an oscilloscope. The number of peaks above the threshold level were counted as electron signals. The detection efficiency was found in this way to be only 20% (26).

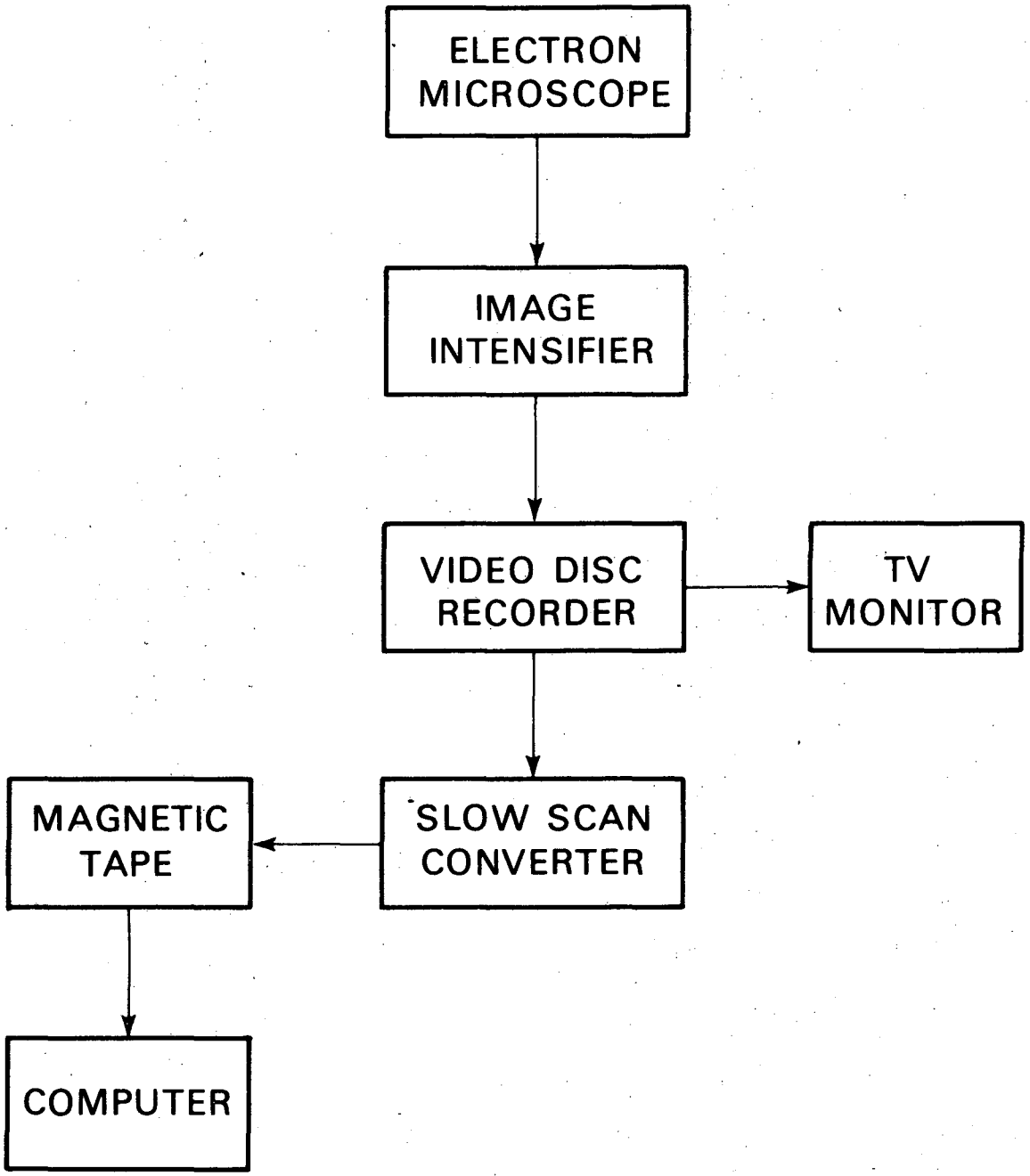

XBL 753-4790

Fig. 3 Diagram of the image intensifier system

A carbon replica of an optical diffraction cross-grating with a period of 54800 lines per inch (purchased from Pelco) was imaged at a magnification of 1600 and an exposure of 3×10^{-4} electron/μm^2. The image data were digitized as described above, and stored on a magnetic tape.

3.3 Computer processing of image data

Processing of statistically noisy images of periodic specimens was carried out on the CDC 7600 and 6600 computers at the Lawrence Berkeley Laboratory. Figure 4 shows the flow diagram of the SNAP-shot data processing system. Using the 7600, digitized data were read in from magnetic tapes into a 2-D array of image intensities. The Fourier transform of the array is generated using the Radix Mix algorithm, described by Singleton (39). This recently developed algorithm removes the restriction that the dimension of the array should be powers of 2; furthermore, an array of odd dimensions can also be transformed. At present, the computer program developed for this thesis is capable of Fourier transforming an array of 320 x 320 points, giving the amplitudes and phases of the diffraction pattern.

Due to the periodicity in the specimen, there will be diffraction spots of high intensity rising above the noise level. To ensure unambiguous determination of the Fourier peak positions, we employ an interactive-display system im-

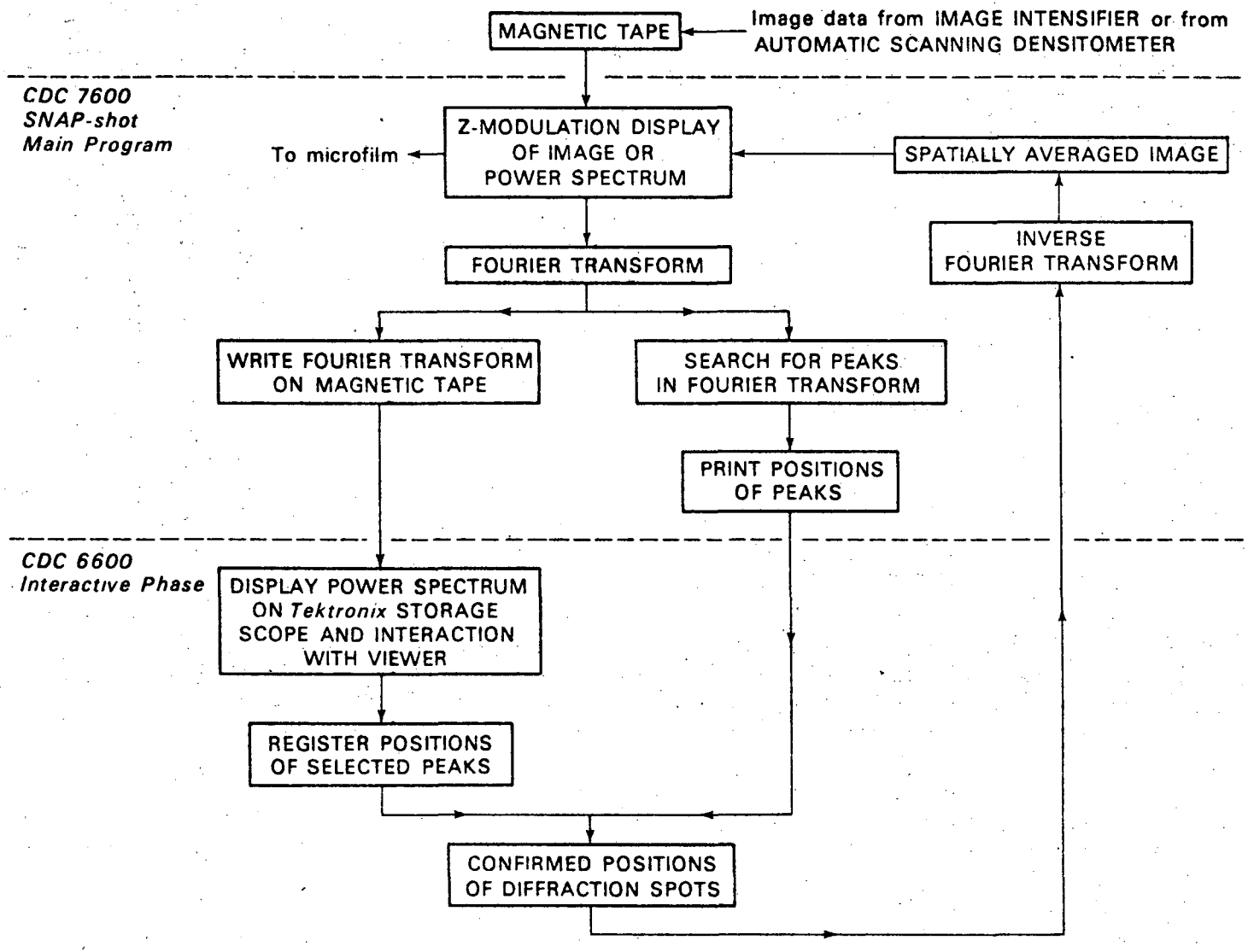

Fig. 4 Diagram of Computer Processing System

XBL 753-4789

plemented on the CDC 6600. Viewing the power spectrum on a Tektronix storage scope (Model 4010), one can select the desired peaks by moving an x and y cursor, so that two lines intersect over the point of interest. Hitting a specified key on the keyboard causes the position of the peaks to be registered. The coordinate numbers thus obtained are compared with those generated by a separate subroutine in the 7600 program which searches for Fourier peaks, and lists them in decreasing order, according to the peak values. This combined approach is especially useful when there are numerous peaks.

Spatial averaging is done by setting the value of each diffraction spot equal to the average of all points within an area chosen around the spot, and setting to zero all other points. The diffraction pattern is then inverse Fourier transformed to give a spatially averaged image.

The computer processing time for Fourier transforming a 320 x 320 array, going through the interactive phase, and spatial averaging amounts to 50 seconds in the 7600 and 10 seconds in the 6600, at a total cost of $US 25.00.

Z-modulation display of the original noisy image, its calculated power spectrum and the averaged image (figure 5) can be plotted on 35mm film via the computer program using a CRT plotting device, the VISTA 250. At every element of the array, the intensity is converted to a discrete number

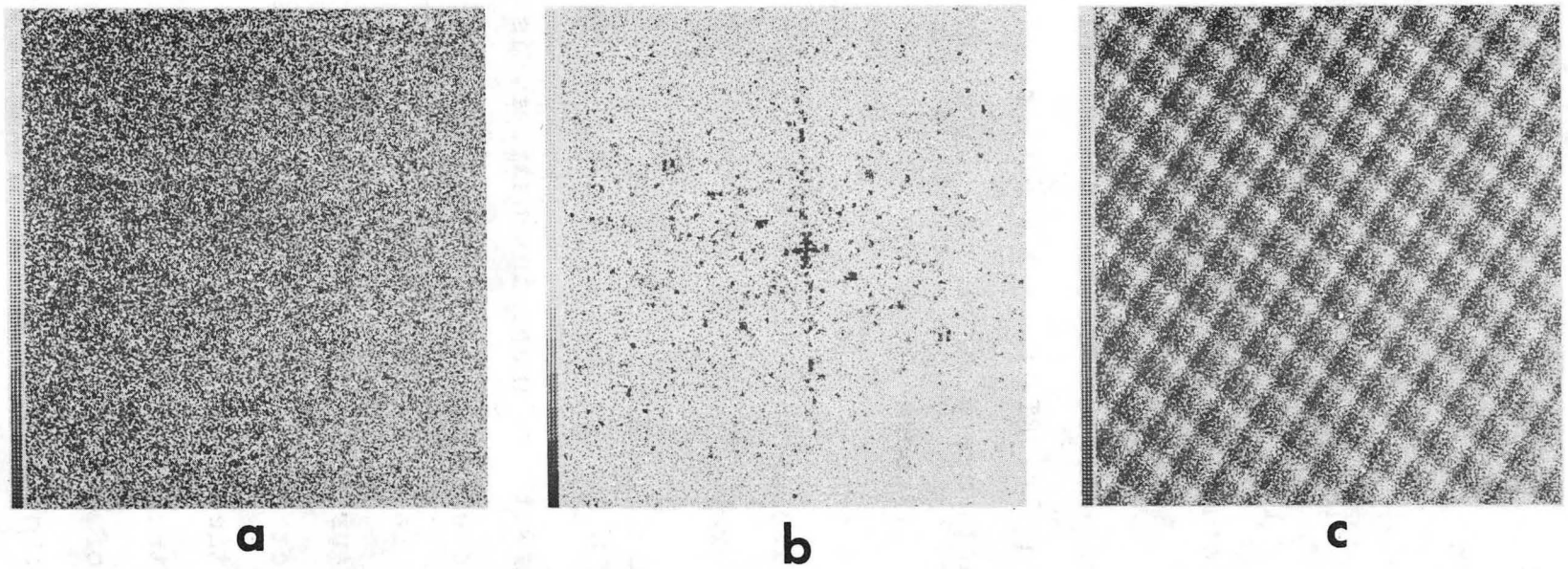

XBB 751-54

Fig.5 a. The Z-modulation display of a statistically noisy image of a carbon replica of an optical diffraction grating, recorded with an image intensifier; b. power spectrum of the statistically noisy image; c. the spatially averaged image.

of grey-levels, and for each unit of greyness, one dot is plotted onto the film. The dot is situated randomly within the corresponding picture element. The VISTA is capable of plotting 1024 x 1024 points. In the display of a 128 x 128 array, one picture element occupies an area of 8 x 8 points. In this case, one expects a maximum of 64 grey-levels. Unfortunately, due to a certain amount of spreading in the dots on the CRT, an 8 x 8 picture element is saturated after 16 dots are plotted, so only 16 grey-levels can be realized. Of course, one can always display an array of a smaller number of picture elements, thus increasing the allowed size of the picture element and thereby the attainable grey-level.

3.4 Results with the image intensifier

The computer display of the noisy image of a cross grating, recorded with an image intensifier, is shown in figure 5a. The power spectrum was calculated and displayed (figure 5b). Figure 5c is the averaged image. The array size for these figures is 128 x 128. Due to the low contrast of the object and the small signal to noise ratio in the image intensities, the calculated values for the peaks in the power spectrum are very weak, and do not even appear in a normal mode of display. An enhancement procedure in the computer program was used to make the location of these low value peaks visible. The enhancement routine involves

the following steps:

(1) Set all elements in the array that are above a threshold value to be equal to this threshold value.

(2) For every array element, apply a non-linear relationship between its grey-level and the actual number of dots plotted: Number of dots plotted for the ith element =

$$\left(\frac{\text{grey-level at the ith element}}{\text{maximum grey-level}}\right)^{N} \times \text{maximum grey-level},$$

where N is a positive integer. We find that the larger N becomes, the more noise is suppressed in the display. In figure 5b, N was set to 4. The accompanying grey-scale illustrates the effect of such an operation.

The averaged image shown in figure 5c was obtained by including the 5 conjugate pairs of diffraction spots and the zero order term in the inverse Fourier transform.

3.5 Evaluation of the image intensifier as a SNAP-shot recorder

Analysis of noisy data collected by an image intensifier demonstrated that spatial averaging is possible. However, the use of an image intensifier cannot be easily extended to higher resolution work. The limiting factors are:

(1) It is clear that for a given critical exposure, statistics can only be improved by averaging a large image area. At present, the window size of the image intensifier is limited to 1 inch in diameter.

(2) With an efficiency of only 20%, too many of the signal electrons are lost.

(3) Distortion of the image by the field aberrations within the television camera, which introduces a spreading of the diffraction spots, can produce artifacts in the averaged image. This artifact is present in the averaged image of a carbon grating (fig. 5c).

CHAPTER 4

PHOTOGRAPHIC EMUSIONS

Valentine (52) found that the photographic emulsion is a very good recording medium for the electron image, in that every silver halide grain hit by an electron is rendered developable. An ideal emulsion for our purpose would be one that has a developed grain size between 10 μm and 25 μm in diameter, and a value of DQE equal to 1. On such an emulsion, one electron would create a developed area sufficiently large to be detected by a scanner with a 25 μm spot size. Such an emulsion would serve as an "image intensifier" with 100% efficiency. A few of the commercially available fast emulsions were investigated.

4.1 Determination of grain size and fog level

Unexposed photographic emulsions were developed and grain sizes were measured under a light microscope. Table 2 lists the various emulsions selected for study, the developing conditions, and the resulting grain size observed. Fresh developer was used in all cases. The fog level of an emulsion was determined both by measuring the optical density of the unexposed area and by counting the number of fog grains in an area of $(100\ \mu m)^2$. Results are listed in Table 2. Figure 6 shows the developed grains in the emulsions studied.

No screen X-ray film (NSX) and Royal-X Pan film (RX)

TABLE 2

Emulsion (Abbreviation) and Developer	Development Time (minute)	Temperature °C	Grain Size (micron)	Fog Count* in $(100\mu m)^2$	Fog Optical Density
1. Kodak Electron Image Plate (EIP) HRP(1:4)+Antifog	5	20	<1	50	<0.1
2. Kodak Blue-Brand Medical X-ray Film (MX) HRP(1:4)+Antifog	1	20	2-4	120	0.1
3. Kodak No Screen X-ray Film (NSX) Kodak Liquid X-ray Developer	7	20	2-10	280	0.4
4. Kodak Royal-X Pan Film (RX) DK-50	6	20	2-10	240	0.4
5. Kodak Nuclear Track Emulsion (NTB2) D-19	10	20	0.26**	-	<0.1

*Values given are only a rough estimation

**Taken from Kodak Technical Pamphlet No. P-64

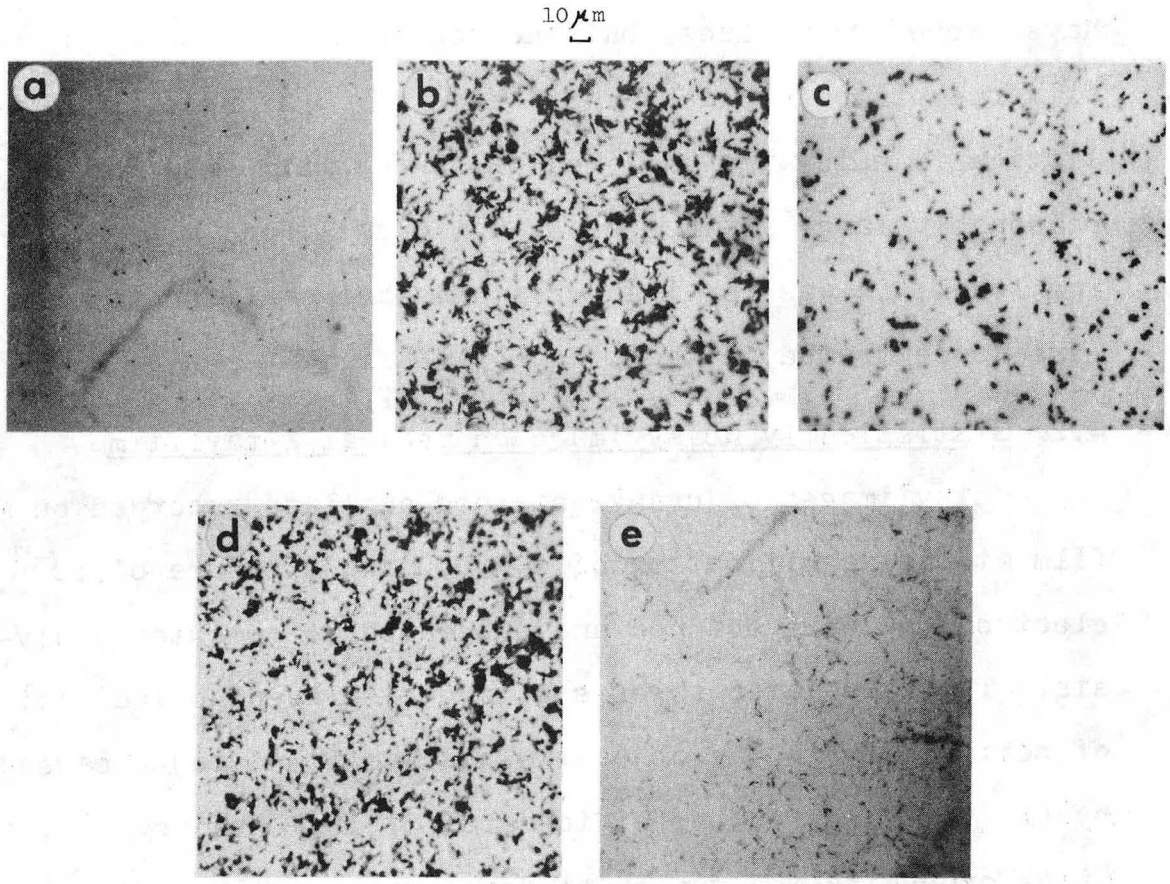

XBB 751-59

Fig. 6 Fog grains in the emulsions studied.
a. Kodak Electron Image Plate;
b. Kodak No Screen X-ray Film;
c. Kodak Blue-Brand Medical X-ray Film;
d. Kodak Royal-X Pan Film.
e. Kodak Nuclear Track Emulsion (type NTB2).

have large grain sizes, but the fog levels are so high that either emulsion would be inefficient as a recorder of statistically noisy images. Medical X-ray film (MX) has a reasonably large grain size (2-4 microns), and a tolerable fog level; it was for these reasons that earlier efforts were concentrated on the study of MX film.

4.2 Statistically noisy image on medical X-ray film

Noisy images of uranyl-stained catalase recorded on MX film at the magnification of x40,000 and exposure of 10^{-3} electron/μm^2 were scanned and subjected to computer analysis. The calculated power spectrum displayed no indication of periodicity in the object. This was found to be caused by (1) the large number of fog grains (10^{-2} grains/μm^2), a value exceeding the number of developable grains resulting from the electron exposure. (2) The grain size was too small, and the scanner was incapable of detecting a change in optical density on the film due to only one electron event.

4.3 Removal of fog grains in medical X-ray film

Additive noise from the image recorder introduces error in the calculated values of the diffraction spots. Furthermore, the weaker diffraction spots may be "buried" in the noise and cannot be recognized. For these reasons, various methods have been tested for their effectiveness in removing the developed fog grains in the MX film:

1. Antifog was added to the developer, but there was no noticable reduction in the total number of fog grains; instead, it caused a reduction in the developed grain size.
2. Based on the assumption that the fog grains might be due to grain-surface latent image specks, formed during manufacturing and aging of the film, the MX film was subjected to bleaching (43) with an acid dichromate bleach ($K_2Cr_2O_7$ 1.9 gm/l, H_2SO_4 1.25 gm/l) for 1 minute, followed by a 30 minute wash in running water. The film was air-dried and dessicated with P_2O_5 in vacuum before use. It was noted that photographic emulsions tend to have increased fog level if the conditions of drying were not optimal. We found that a condition of fast drying and low humidity was favorable. In addition, special care was taken to minimize stresses and movements of the emulsions. Nevertheless, streaks of dense fog were often found on the developed films. The advantage of bleaching, if any, was more than offset by the creation of the new fog.
3. MX film has emulsion coated on both surfaces of the acetate sheet support. The emulsion on the bottom surface of MX film contains a high level of fog, caused partially by secondary radiation generated during exposure in the microscope. After exposure in the electron microscope, the bottom layer emulsion was removed by placing it in close contact with a piece of blotting paper saturated with Kodak

fixer. After 5 minutes of fixing, the film was washed for 5 minutes, and developed.

In the subsequent experiments, the Medical X-ray films used were not bleached before exposure in the electron microscope, but the bottom emulsion layers were always removed just before development. The problem of detecting single electron events by a scanning microdensitometer still remains. In the following section, we investigated the possibility of amplifying the electron signals by infectious development (41).

4.4 Infectious development of medical X-ray film

It was found that when hydrazine compounds were added to alkaline developers, previously unexposed silver halide grains in the vicinity of the exposed grains became developable (41). This effect was termed "infectious development". We experimented with infectious development on Medical X-ray film using Kodak developer D-8, varying the amount of hydrazine dihydrochloride ($N_2H_4 \cdot 2HCL$) in the developer. When the concentration of hydrazine was 0.25 gm/1000 cc, clusters of grain ranging from 10-25 microns in size were formed (figure 7a). Development proceeds rapidly at room-temperature, and was completed within 15 seconds. The progress of development can be monitored visually by observing the amount of darkening under a safelight (Kodak safelight filter No. 2, dark red). Development was stopped

10 μm

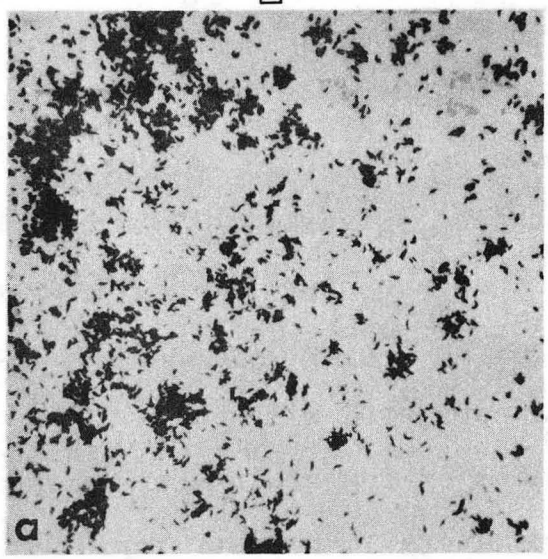

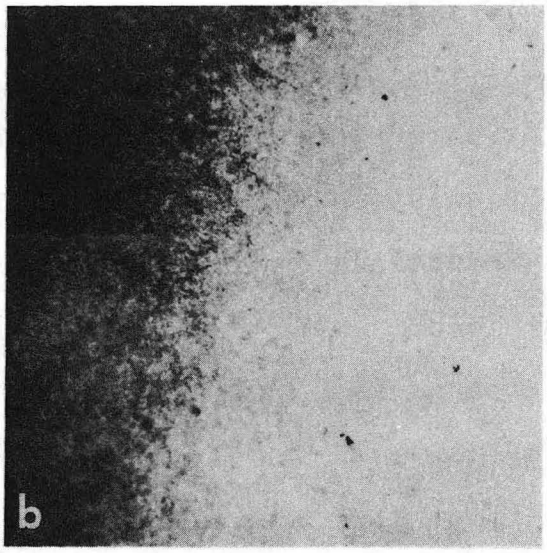

XBB 751-52

Fig 7 a. Infectiously developed Kodak Medical X-ray film. The right half of the picture represents area unexposed to electrons. b. Infectiously developed Kodak Nuclear Track Emulsion (type NTB2). The right half of the picture represents area unexposed to electrons; the left half had been exposed to 10^{-5} $e^-/\mu m^2$.

when the optical density was estimated to reach a value between 1 to 2. By developing at 10°C, the time of development can be lengthened slightly to 1 minute. Inherent fog grains also served as a center for infectious development, and this is evident in figure 7a, where the unexposed area of the MX film is populated with many grain clusters. In general, development of fog grains can be suppressed by lowering the temperature. However, for MX film, when it is infectiously developed at 10°C, there was no noticeable reduction in the number of grain clusters (fog) in the unexposed area (figure 7a).

The major obstacle in choosing larger grain emulsions (NSX, RX and MX) as a recording medium of statistically noisy images is the existence of inherent high fog level in these emulsions. Infectious development was also tried on smaller grain emulsions. On EIP, a developing condition for the clustering phenomenon was not found. Preliminary results with Kodak Nuclear Track Plates, type NTB2 (25 micron emulsion thickness), indicated a favorable outcome; a more detailed discussion of NTB2 emulsion is presented in the next chapter.

4.5 The use of phosphorescent screens to amplify the electron signals

Phosphorescent materials emit photons upon excitation by energetic electrons. The possible use of these mater-

ials as electron signal amplifiers was tested with zinc sulfide and plastic scintillators. Photographic emulsions (EIP and MX film were used) partially covered by ZnS or plastic screens, were exposed to 4×10^{-3} electrons/μm^2 in the electron microscope. After development, the optical densities of different areas of an image plate were recorded and compared. A higher optical density value in the area directly beneath the phosphorescent screen would indicate that the screen can be useful as a single electron signal amplifier.

Zinc sulfide screens were prepared by the following method: A measured quantity of zinc sulfide (Type GN3P, Levy West Laboratories Ltd., Harlow, England) was added to a solution of iso-amyl-acetate ($CH_3COO\ C_5H_{11}$) containing 10% collodion. The suspension was poured into an evaporating dish, and the phosphore was allowed to settle onto a glass cover slip placed at the bottom of the dish. The solution was allowed to evaporate over a period of 24 hours, leaving a thin film of the desired thickness on the glass. Screens of 40, 26, 10, and 5 mg/cm^2 thicknesses, were prepared in this manner.

Results from using ZnS screens of different thicknesses on MX films are listed in Table 3. For an initial exposure of 4×10^{-3} electrons/μm^2, the highest optical density measurement, 0.65, was taken from an area directly

TABLE 3

Optical Density Measurements on Medical X-ray Films with the Use of ZnS Screens

Screen Thickness (mg/cm^2)	40	26		10		5	*
Exposure (electrons/μm^2)	$4x10^{-3}$	$4x10^{-3}$	$4x10^{-3}$	$2x10^{-3}$	10^{-3}	$4x10^{-3}$	$4x10^{-3}$
Optical Density	0.25	0.4	0.65	0.35	0.25	0.4	0.3

*Measurement taken from an area not covered by the screen.

beneath a screen 10 mg/cm^2 thick. Compared to the optical density in the area not covered by a screen, there was a 2-fold increase in the optical density. Thus, the optimum thickness of the ZnS screen was taken to be 10 mg/cm^2.

Using a 10 mg/cm^2 thick screen, the amplification of electron signals was tested, on MX film, at decreasing exposures (table 3). At 2 x 10^{-3} electrons/μm^2, the measured optical density just beneath the screen was about equal to that of the unscreened area of the film. At 10^{-3} electron/μm^2, the density was less than that of the unscreened area. This last result must be accounted for by the fact that electrons do not penetrate the screen, and also by the fact that the small number of photons generated by this level of electron exposure is not enough to render silver halide grains in the emulsion developable, a phenomenon due to reciprocity law failure of photographic emulsion (30).

Experiments using a 10 mg/cm^2 ZnS screen on the Electron Image Plate exhibited no evidence of increased optical density in the area covered by the screen, when the exposure was 4 x 10^{-3} electrons/μm^2. Results from using plastic scintillators of different thicknesses on both MX film and EIP were negative.

From the above discussions, we concluded that, provided the electron exposure at the image plane is not lower than 4 x 10^{-3} electrons/μm^2, a ZnS screen of appropriate

thickness can be useful as an electron signal amplifier. When it becomes necessary to operate at an exposure less than 4×10^{-3} electrons/μm^2, an alternative method must be used.

CHAPTER 5

KODAK NUCLEAR TRACK EMULSION (TYPE NTB2)

Kodak NTB2 plates have a DQE value of 1 at high electron exposure (0.13 electron/μm^2 - specified in the Kodak data release sheet). When processed in the manner recommended by the manufacturer, 80 Kev electrons form tracks between 10 μm and 25 μm in length. If developed infectiously, clusters of grains were formed. It has been found that hydrazine compound, added to an alkaline developer such as D-8, induces development of unexposed grains in the vicinity of exposed grains (41). One can conclude that the grain clusters noted in the NTB2 emulsion are the result of local fogging in the vicinity of a developed track (figure 7b). For exposures of 10^{-3} electron/μm^2 and lower, it is necessary to suppress undesirable fogging by carrying out the development at a temperature as low as $4^{o}C$. Under this condition, the background can be kept to a very low level (figure 7b, 8).

Due to difficulties encountered with long delivery times, the frequent presence of cosmic-ray tracks (figure 6e), and the high cost of Kodak manufactured NTB2 plates ($3.13/plate), subsequent experiments have so far been carried out with photographic plates prepared in our laboratory. Gelatin coated glass plates prepared in advance were used for coating the emulsion. The gelatin coat is

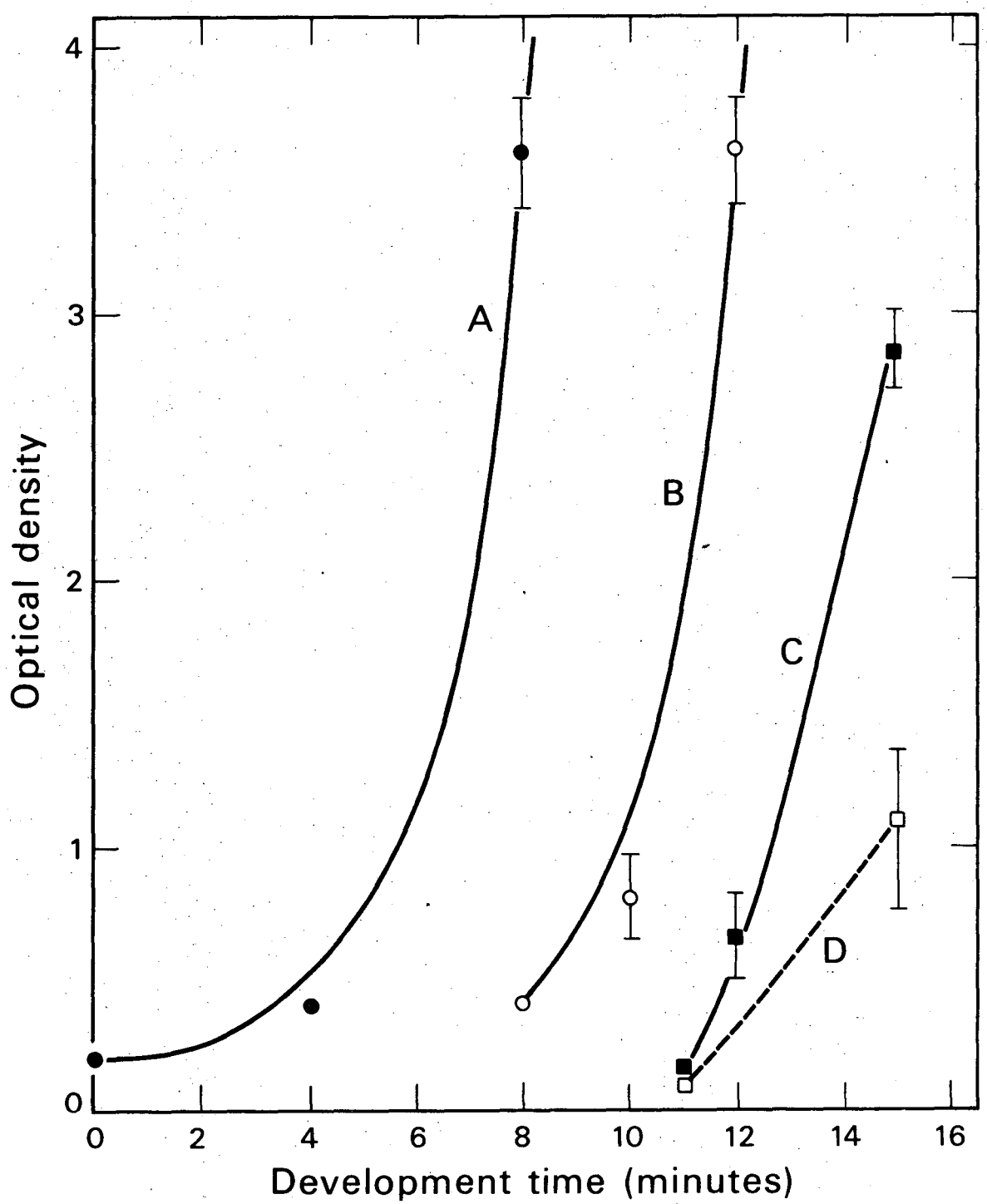

XBL 753-4793

Fig. 8 Optical density of NTB2 emulsion plotted against the time of infectious development. The NTB2 plates were subjected to different levels of electron exposure. A. 10^{-2}electron/μm^2; B. 10^{-3}electron/μm^2; C. 10^{-4}electron/μm^2; D. fog.

necessary in providing firm adhesion between the emulsion and the glass. The choice of gelatin often affects the emulsion sensitivity and fog level (4); therefore, it is essential that only photographic gelatin be used for this purpose.

Procedure for preparing gelatin coated glass:

(1) Add 5 gm of Ilford photographic gelatin to 200 ml of distilled water.

(2) Let the gelatin gradually swell in the water; this takes about 2 hours. The swelling period is necessary for gelatin to completely dissolve in the water.

(3) Add distilled water to reach a total volume of one liter.

(4) Add 25 ml of 3% Potassium Chrome Alum, and 4 drops of Kodak Photoflo 200 to the gelatin solution.

(5) Place the mixture in a hot water bath (about 60°C), and stir gently to avoid forming bubbles.

(6) Dip a cleaned 4" x 3¼" glass plate into the warm solution.

(7) The gelatin coated glass is then removed and air-dried on a rack.

Procedure for coating NTB2 emulsion:

The emulsion can be purchased from Kodak in 4 oz. bottles. The emulsion is first melted in a 37°C water bath for 1 hour, and the gelatin coated glass plates are warmed

to 50°C on a hot plate before coating with emulsion. Then the following steps are carefully executed:

(1) Balancing a glass plate with one hand, pour approximately 10 cc of melted emulsion onto the center of a gelatin coated glass plate. The plate is then tilted slowly in all directions so that the emulsion reaches all four corners. This is followed by draining the emulsion back into the container, so that only a very thin film of emulsion is left on the plate. This step is important to ensure even spreading of emulsion in the following operation.

(2) Pour 2 cc of emulsion onto the center of the glass plate, tilting the plate in all directions until it is evenly coated with the emulsion.

(3) The coated plate is then air-dried on a level surface in a dust-free environment.

(4) This is followed by dessicating the plates thoroughly with dessicator (type humi-cap, Driaire Incorp., Conn.) for two days in a light tight box. Plates are again dessicated in vacuum with P_2O_5 before use.

To determine the emulsion thickness of these plates, an unexposed plate was developed and examined under a light microscope. Imaging on the gelatin layer, the amount of defocus in going from the gelatin-glass interface to the gelatin-air interface was determined. This value was then

compared to that of a Kodak manufactured NTB2 plate of 25 μm thickness. The emulsion thickness for the home-made plate was also found to be approximately 25 μm.

Procedure for infectious development of NTB2 emulsion:

(1) Develop first in D-19, at 10°C, for 20 minutes.

(2) Immediately transfer the plate to D-8, which is maintained at a temperature of 4°C. Hydrazine dihydrochloride ($N_2H_4 \cdot 2HCL$), in the amount of 0.25 gm/1000 cc, has been added to the D-8 developer to cause infectious development.

(3) The time of development in D-8 varies with the exposure. The progress of development is closely followed by observing the gradual darkening of the emulsion under a safe light (Kodak safe light filter No. 2), and it is stopped when the emulsion reaches an appropriate darkening that corresponds to a developed optical density between 1 and 2. The time of development is much longer than that of Medical X-ray film, therefore termination of development can be controlled more accurately (figure 8).

(4) The plate is then rinsed in running water for 30 seconds; prolonged washing causes an increase in the fog level.

(5) Fix in Kodak fixer for 15 minutes, and wash for 1 hour.

Developer containing hydrazine compound oxidized rapidly;

therefore it is made up immediately before use and is not stored or reused. An infectiously developed NTB2 plate, exposed to 10^{-3} electron/μm^2, is shown in figure 7b.

5.1 Electron Microscopy

Experiments were performed on a JEM 100B electron microscope, operating at 80 Kev. The exposures were measured at a plane just below the photographic plate, using a lithium-drifted silicon detector. The detector counting efficiency has not been determined accurately; when compared to the readings from a Faraday cage, it was found to be approximately 80% efficient (22). We have not corrected for the counting efficiency in the data presented here.

A condition of low beam current was achieved by using a moderately small condensor aperture (200 micron), and setting the bias to the lowest possible value. During the recording of statistically noisy images, the field limiting aperture was used to protect one area of the image plate from the electron beam, so that the fog level could be assessed for each individual plate.

Commercial preparation of bovine liver catalase (C.F. Boehringer & Soehne, Mannheim) was recrystalized by the method described by Wrigley (54). A drop of catalase crystals in suspension was placed on top of a formvar coated grid, and the crystals were allowed to settle on the film. The excess solution was drained off, and a drop of aqueous

2% uranyl acetate was added. The stain was left on the grid for 1 minute, and excess liquid was drained off thoroughly to prevent build up of stain around the protein crystal. The grid was coated with a thin layer of carbon film (about 100 Å thick) to prevent specimen charging.

5.2 Optical diffraction and microdensitometry

Optical diffraction patterns of images of uranyl stained catalase are obtained on an optical bench that has been assembled in-house and features a neon-argon laser beam that is expanded to a diameter of 2 inches. Due to the aberration of lenses along the laser path, only an area 1 inch in diameter in the center of this field is useful for diffraction. Diffraction patterns were recorded on Polaroid films with a Graflex camera.

Optical densities of developed NTB2 plates were measured with a Joyce Loebl Microdensitometer, Model MK IIIC. Owing to the low exposure and the infectious development, the emulsion exhibited considerable graininess, causing a large fluctuation in the optical density readings.

Photographic images were also scanned with an automatic microdensitometer, assembled by the Remote-sensing research group of the University of California, Berkeley. Scanning spot size was estimated to be 25 μm. Digitized data were recorded on magnetic tapes for processing in the computer, as described in chapter 3.

5.3 Signal amplification and noise suppression on the NTB2 emulsion

The effect of infectious development on signal and noise can best be studied from an optical density versus development-time plot (figure 8). Data were obtained from Kodak NTB2 plates. The plates were subjected to varying electron exposures in the electron microscope, with no specimen in the beam. A field limiting aperture was used to block electrons over one area of the plate, from which the background fog levels could be determined. For exposures of 10^{-2} and 10^{-3} electron/μm^2, when the densities in the exposed areas were developed to values as high as 3.6, the fog level remains unchanged. It is also interesting to note that there is a good signal to noise (fog) discrimination even for exposures as low as 10^{-4} electron/μm^2 (figure 8).

5.4 Grating resolution of NTB2 emulsion

The point resolution of an emulsion is normally determined by finding the smallest distance between two points that can be resolved. This procedure cannot be applied to a statistically noisy image. An objective way of determining resolution would be to image a periodic object of high contrast and small repeat distance. The highest resolution spot in the diffraction pattern then corresponds to the emulsion resolution. Not to be confused with

point resolution, the value thus obtained is referred to as "grating resolution" in this thesis. Uranyl-stained catalase is a satisfactory specimen for this purpose, although using a specimen of higher contrast might yield smaller values for the grating resolution. It should be stressed that emulsion speed is usually increased at the expense of degrading the emulsion resolution.

Resolution of infectiously developed NTB2 plates varies with the electron exposure. To determine the emulsion resolution, uranyl-stained catalase was imaged at different exposures, followed by infectious development until the optical density reaches a value between 1 and 2. The magnification was chosen such that the available object resolution was always better than the estimated emulsion resolution. The optical diffraction patterns (figure 9) of the catalase images give the values for the grating resolutions. Using the same criteria in all cases, the grating resolution was also determined for both Medical X-ray film and Electron Image Plate (developed in 1:2 HRP for 5 minutes for maximum speed). The results are listed in table 4.

5.5 Present status of experimental results with NTB2

Preliminary work has been undertaken to use NTB2 emulsion for getting SNAP-shot data. Photographic plates coated with NTB2 emulsion were used to record statistically noisy

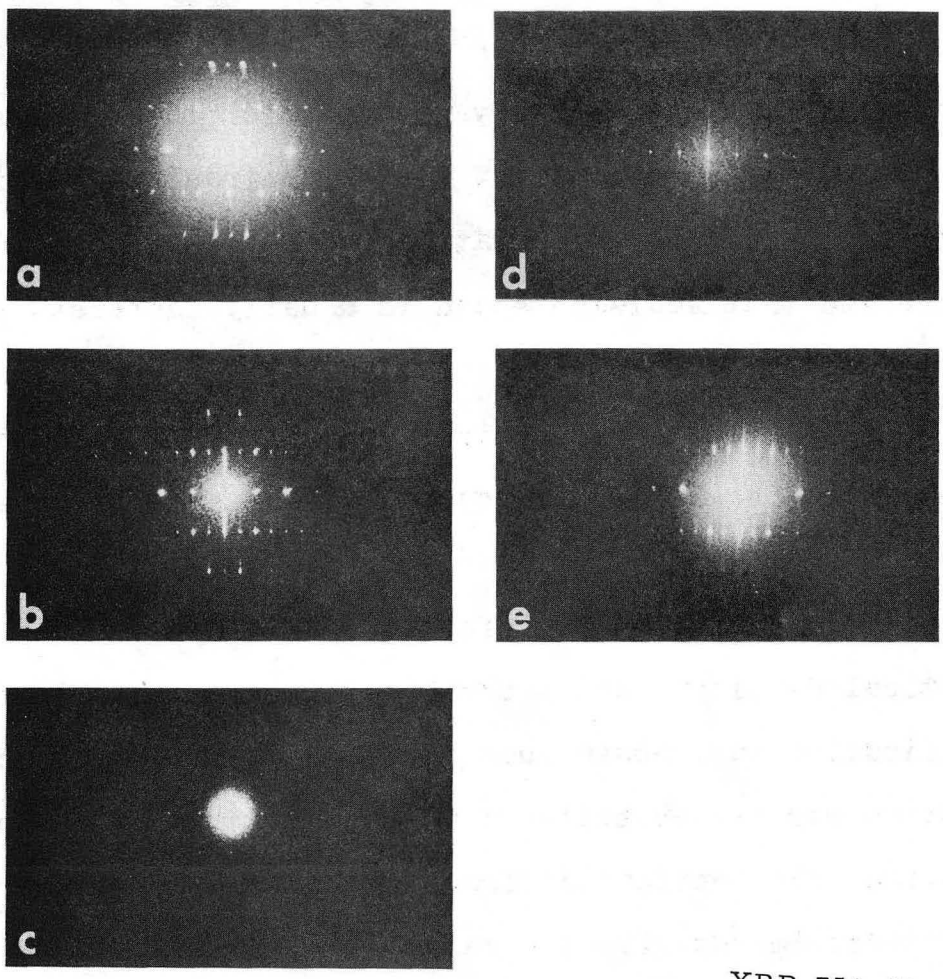

XBB 751-53

Fig. 9 Diffraction patterns of the images of uranyl stained catalase crystals recorded on different emulsions:

a. on NTB2, at the magnification of 10,000, and at the exposure of $4 \times 10^{-2} e^{-}/\mu m^{2}$;
b. on NTB2, at the magnification of 20,000, and at the exposure of $10^{-2} e^{-}/\mu m^{2}$;
c. on NTB2, at the magnification of 20,000, and at the exposure of $10^{-3} e^{-}/\mu m^{2}$;
d. on No Screen X-ray Film, at the magnification of 10,000, and the exposure of $4 \times 10^{-2} e^{-}/\mu m^{2}$;
e. on Kodak Electron Image Plate, at the magnification of 10,000, and exposure of $0.25 e^{-}/\mu m^{2}$.

TABLE 4

Determination of Grating Resolution of Infectiously Developed NTB2

Emulsion Type	Exposure (electron/μm^2)	Magnification	Grating Resolution (micron)*
EIP (1:2 HRP)	0.25	x10,000	21
NSX	0.04	x10,000	28
NTB2	0.04	x10,000	21
NTB2	0.01	x20,000	43
NTB2	0.001	x20,000	86

*Upper-bound determined experimentally. Limiting grating resolution, especially for high contrast structure, may be smaller than these values.

images of uranyl stained catalase crystals. The technique of microscopy that we used is similar to the minimum beam method (55), except that the specimen exposures never exceeded the value of 3 electrons/$Å^2$. Each exposure was followed by recording the same image area on a Kodak Electron Image Plate. The structural resolution recorded in the images was determined from optical diffraction patterns that were taken from areas 2.5 cm in diameter.

An image of a stained catalase crystal (figure 10a) taken at the relatively high exposure (for NTB2) of $2x10^{-2}$ electron/μm^2, contains high resolution crystalline information out to 10.6 Å. The image appears "statistically defined", even though the emulsion exposure is about 50 times less than the exposure normally used for Electron Image Plates. It is interesting to note, in the optical diffraction pattern (figure 10b), that the support film phase-contrast granularity extends to approximately 5 Å (0.2 $Å^{-1}$). Unfortunately, the corresponding EIP image was not obtained for a direct comparison of image information on the two emulsions. However, the data on the NTB2 plate alone suggests that, by Williams' minimum beam exposure technique, high resolution images can be recorded with reduced exposure if NTB2 plates, instead of EIP, are used.

An image of a stained catalase crystal recorded on NTB2 with much lower exposure is shown in Fig. 11a. It was

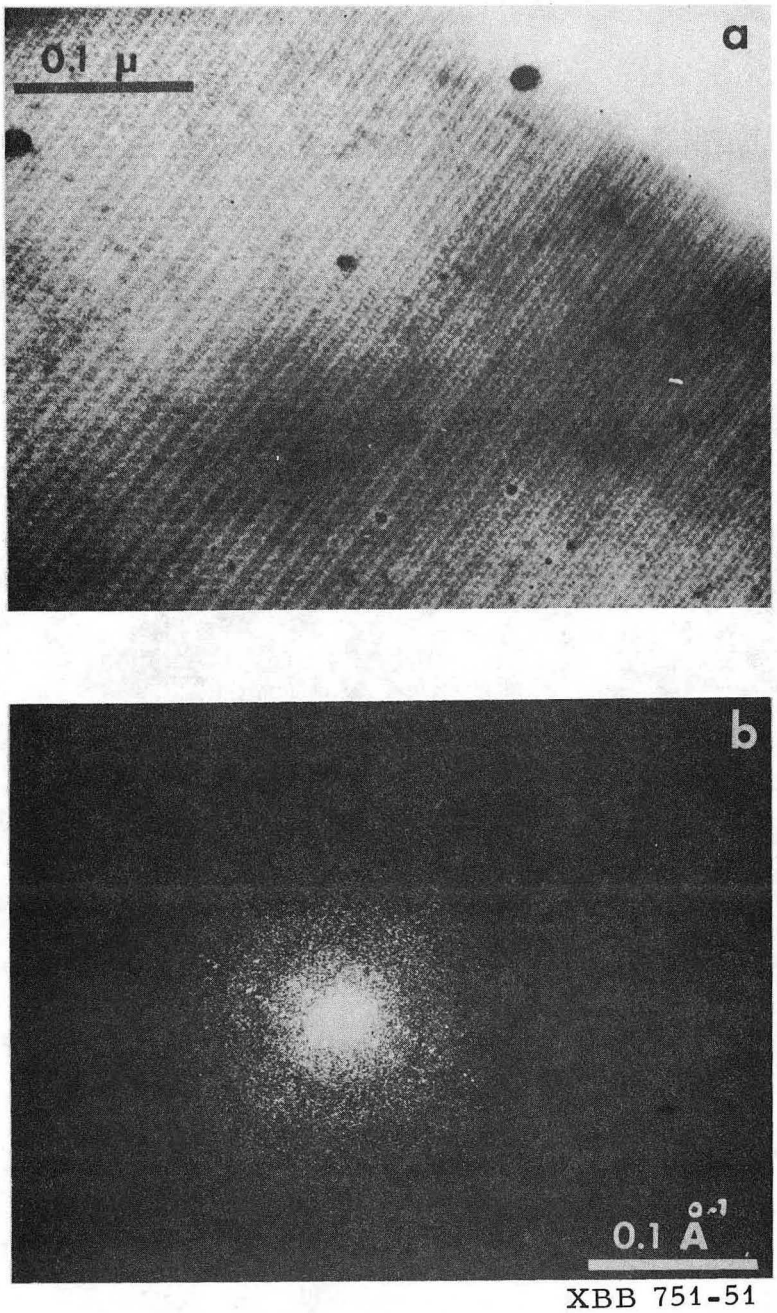

XBB 751-51

Fig. 10 a. Image of an uranyl stained catalase crystal on NTB2, taken at the exposure of 2×10^{-2} electron/μm^2, and at the magnification of 100,000; large black dots are caused by remaining bubbles in the NTB2 emulsion; b. diffraction pattern of the image in fig. 10a.

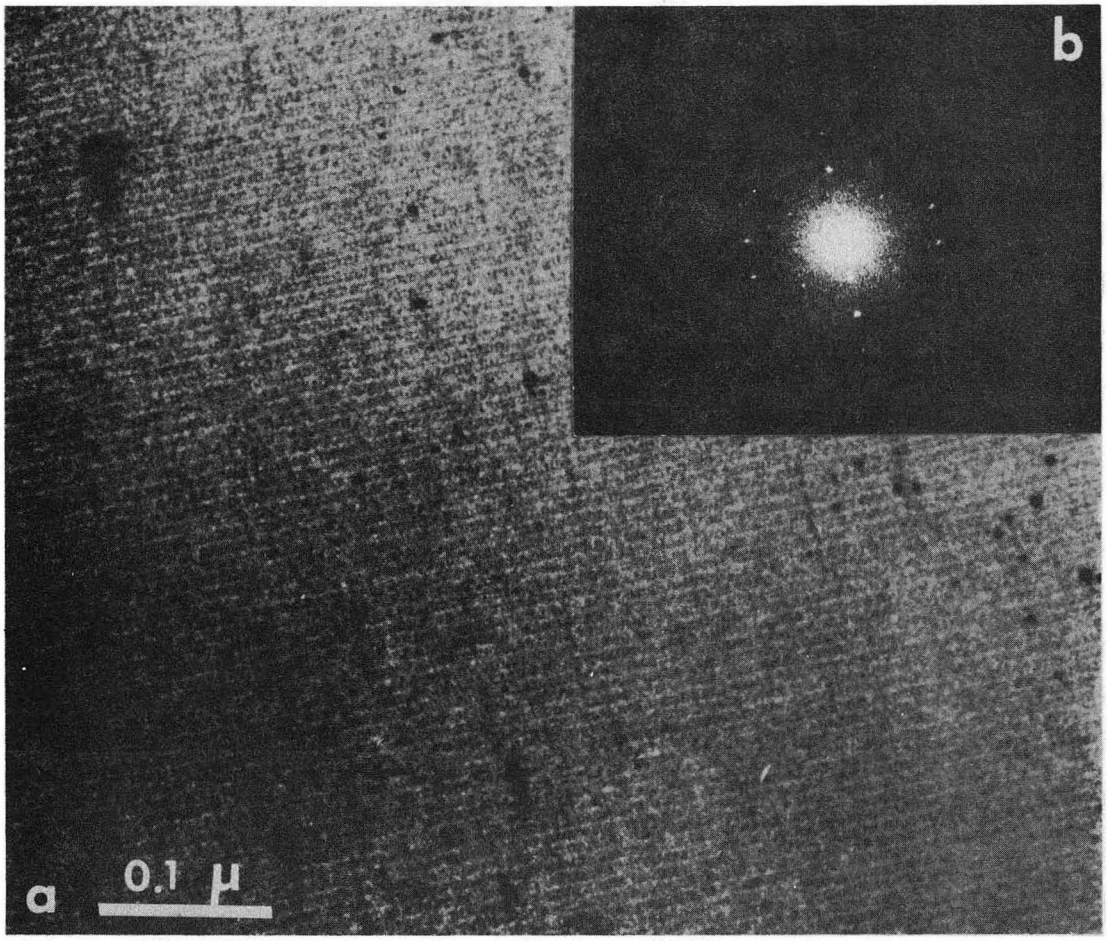

XBB 751-57

Fig. 11 a. The statistically noisy image of an uranyl stained catalase crystal on NTB2, taken at the exposure of 5×10^{-3} electron/μm^2, and the magnification of 40,000; b. diffraction pattern of the image from an area 2.5 cm in diameter.

recorded at the magnification of 40,000 and an exposure of 5×10^{-3} electron/μm^2 at the image plane. Figure 12a shows the same image area recorded on a Kodak Electron Image Plate at an exposure of 1 electron/μm^2. Figure 11b, 12b are the respective optical diffraction patterns taken from identical image areas in the two cases.

Figure 11b indicates a lower resolution even though the specimen was less radiation-damaged. The reason for this, we believe, is that the total number of electrons incident on the NTB2 plate in an area 2.5 cm in diameter is too small to give a high resolution, optical diffraction pattern. To further demonstrate this point, an optical diffraction pattern from a small area, only 3 mm in diameter, of the Kodak Electron Image Plate was recorded (figure 12c). This also shows a lower resolution diffraction pattern. The number of incident electrons included in the image area used to produce Figure 12c is approximately 3 times the number of electrons in the image area corresponding to Figure 11b. Therefore, it seems evident that the resolution present in the optical diffraction pattern of the statistically noisy image could be improved upon by using a larger area for diffraction. We have not yet been able to actually accomplish this directly. The principal difficulty encountered is the irregular stain distribution over different areas of the crystal. Better

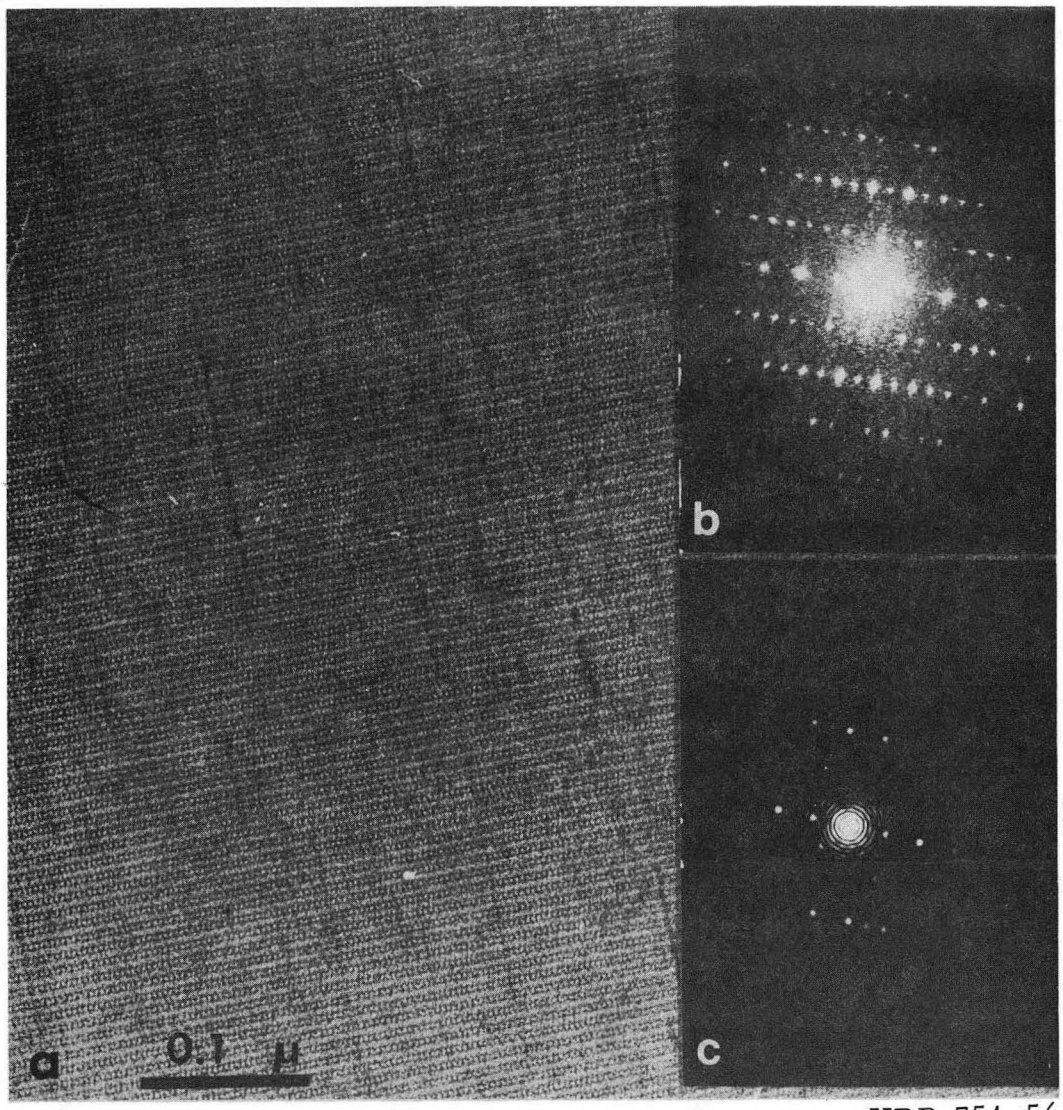

XBB 751-56

Fig. 12 a. Image of the same catalase crystal in fig. 11a. The image is now recorded on a Kodak Electron Image Plate, at the same magnification, but at 1 electron/μm^2. b. Diffraction pattern of the image from an area 2.5 cm in diameter; c. Diffraction pattern from an area 3 mm in diameter.

specimen preparation is necessary to provide specimens with extended areas of ordered, identical unit cells. Nevertheless, we consider the present results to be encouraging, as they demonstrate that the same resolution (in Figure 11b and Figure 12c) has been retreived with 3 times fewer total number of electrons contributing to the data, and at 200 times less exposure to the specimen. In the above experiment, it is interesting to note that, contrary to common belief, the image recorded on a conventional Electron Image Plate is in fact a statistically noisy image. Only after spatial averaging, such as occurs in forming an optical diffraction pattern from a large area, can high resolution data be obtained (Figure 12b).

5.6 Best attainable resolution of the SNAP-shot method using NTB2

The attainable resolution can be considered to vary with the magnification either linearly or inversely, depending upon the two inequalities that are expressed in condition 2.4 and condition 2.6 in Chapter 2. In the case of NTB2 emulsion (after infectious development) the emulsion resolution (p) itself is also an indirect function of the magnification, if the exposure at the specimen is assumed to be held constant. This necessary assumption leads to the obvious consequence that the exposure in the image varies inversely as the square of the magnification; since

the grating resolution of NTB2 increases with decreasing exposures (for constant O.D.), we find the result that the grating resolution is indirectly dependent upon the magnification. Since the attainable resolution (d_s) expressed by condition 2.6 has both an implicit and an explicit dependence on magnification (M), we have calculated d_s for several values of M, and these values are listed in Table 5.

The two equalities that are contained respectively in conditions 2.4 and 2.6 can be plotted as curves of d_s vs. M. These two curves must intersect at a point P, as shown in Figure 13. In this figure, curve A represents the equality $d_s = \frac{5M}{C(rfN_{cr})^{\frac{1}{2}}}$, where C = 0.01, N_{cr} = 1 electron/$\mathring{A}^2$ and f = 1; r is taken to be $\left(\frac{9\ cm}{100\ \mathring{A}}\right)^2$ as previously assumed. Curve B represents the equation $d_s = \frac{p}{M}$, where the implicit dependence of p on M has been taken into consideration: curve B is in fact a plot of the numbers presented in Table 5. The ordinate of the point P, where these two curves intersect, is the best attainable resolution for the parameters and conditions that have been specified. If these parameters are changed, then it is clear that the estimate of the best attainable resolution will also change. In the case represented by the curves in Figure 13, the best attainable resolution when using NTB2 emulsion is estimated to be approximately 4 $\mathring{A}$.

TABLE 5*

Values of magnification, grating resolution, and attainable object resolution used to plot curve B in figure 13.

Magnification M	Exposure (electron/μm^2)	Grating Resolution p (micron)	Attainable object resolution d_s(Å)
10,000	1	20**	20
20,000	0.25	20	10
50,000	0.04	21	4
100,000	0.01	43	4
300,000	0.001	86	2.8

*Assuming N_{cr} = 1 electron/$Å^2$, the actual exposure on the image plate is calculated for each M, and the corresponding grating resolution (p) is found from table 4. Using equation 2.6, the value of d_s for each M is calculated. A plot of d_s vs. M is shown in figure 13.

**Estimated value.

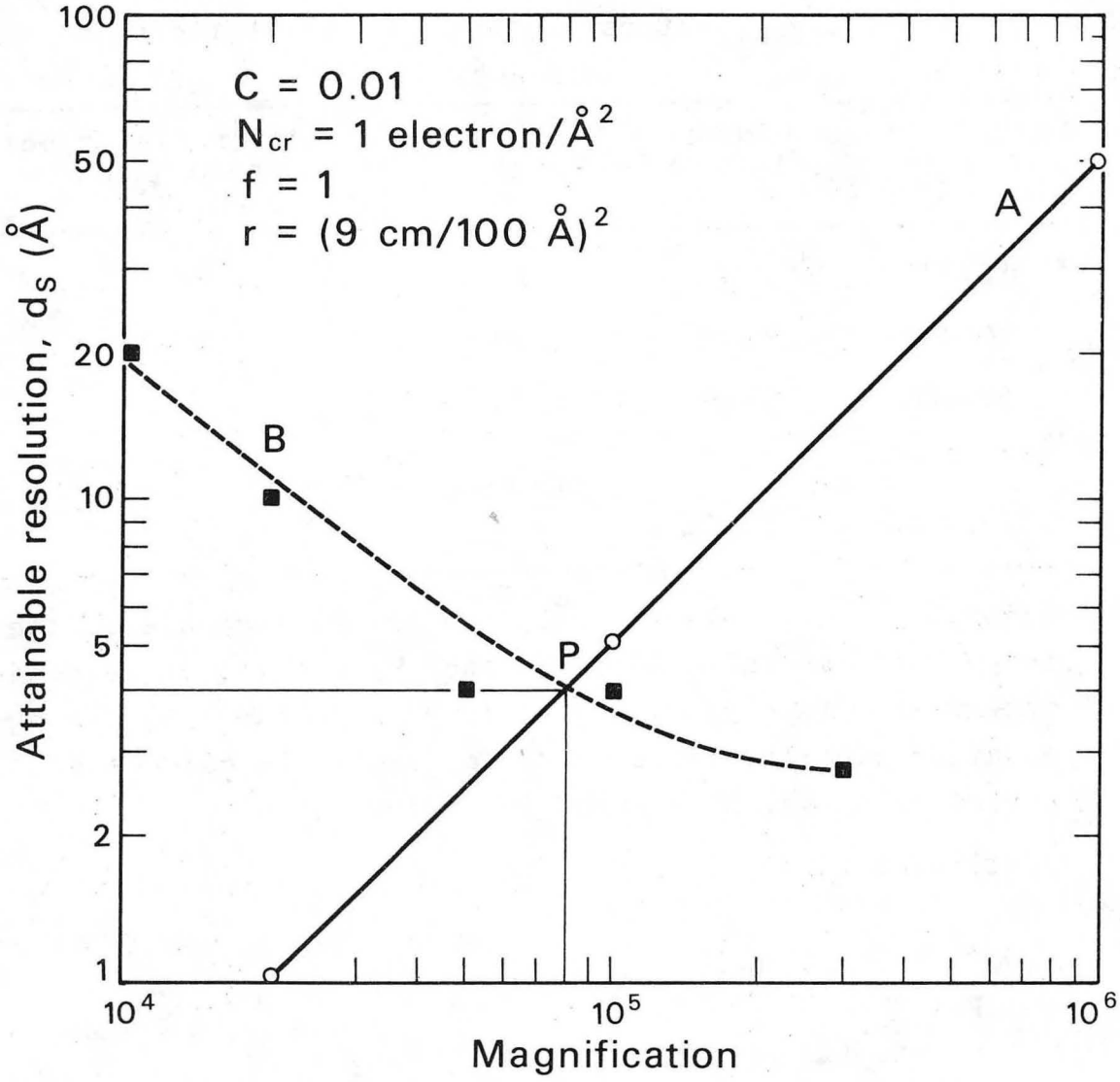

XBL 753-4792

Fig. 13 Attainable resolution vs. magnification. Curve A is a plot of equation 2.4; curve B is a plot of equation 2.6.

5.7 Contrast of infectiously developed NTB2

The dynamic range of a photographic emulsion is the number (g) of distinguishable grey-levels in a resolution element. For a fast emulsion, the dynamic range would be small, while the opposite is true for a slow emulsion. As a result of the smaller dynamic range, the contrast of a fast emulsion would have a higher value. This can be demonstrated by calculating the contrast (C) between two adjacent picture elements, with a difference in optical density exactly equal to Ds/g, Ds being the saturation density. The contrast as defined in section 2.3, will be expressed as

$$C = \frac{(Ds/g)}{\overline{D}} = \frac{D_s}{\overline{D} \cdot g} ,$$

where $\overline{D}$ is the averaged density of the two picture elements; C is found to be inversely proportional to g.

NTB2 emulsion which is given a low exposure and is then infectiously developed will be high in contrast, because it has a reduced dynamic range. Figure 14 shows an image of a stained catalase crystal on NTB2, taken at the exposure of 0.2 electron/μm^2. The large density difference between the crystal and the support film, and the distinct appearance of a layer structure on the crystal are the manifestation of the high contrast produced with infectious development at low electron exposure.

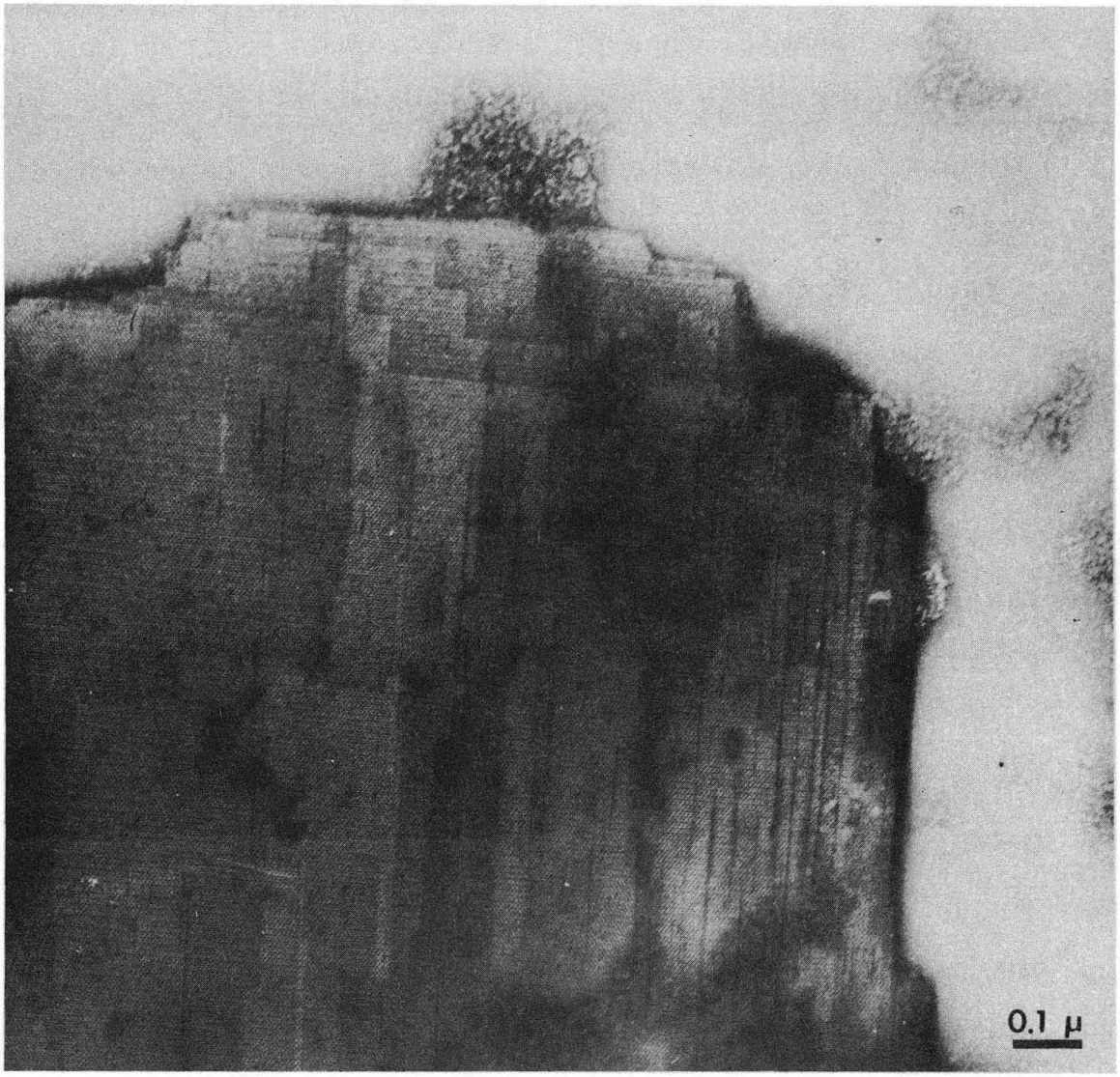

XBB 751-58

Fig. 14 Image of an uranyl stained catalase crystal recorded on NTB2 emulsion, at the magnification of 40,000, and the exposure of 0.2 electron/μm^2.

5.8 Evaluation of the NTB2-Infectious development approach

The advantages of the NTB2-infectious development method are the following.

(1) Large image areas (as large as the size of the image plate) ought to be included in the averaging.

(2) The image is relatively free of distortion, so that the periodicity of the structure can be preserved in the spatial averaging process.

(3) High electron detection efficiency and low fog levels are attained.

(4) The emulsion is capable of a fairly wide range of response to varying electron exposures.

(5) Matricardi et al. (29) reported improved sensitivities of No Screen X-ray film, and images were recorded with exposures as low as 4×10^{-2} electron/μm^2. The background O.D. was found to be 0.4. For the same exposure, NTB2 has a smaller grating resolution, and the background O.D. is undetectable. This causes NTB2 to have a greater dynamic range than NSX.

(6) NTB2 emulsion has high contrast values, even at very low exposures.

At the present state of the art, some of the disadvantages are:

(1) Unless the number of electrons incident on the plate is known accurately, the time of development in D-8

cannot be pre-determined. Progress of development must be monitored visually. This means that image plates have to be treated individually.

(2) The gain in sensitivity also enhances the disturbing effects of irregularities in the emulsion, such as stress marks due to irregular drying, and variations in the emulsion thickness.

Due to the quality of the NTB2 plates prepared in our laboratory, we are limited at present by the plate irregularities and fog level to exposures of the order of 10^{-3} electron/μm^2. Preliminary results with Kodak NTB2 plates indicated that the prospect of recording at 10^{-4} electron/μm^2 or lower is very good.

5.9 Discussion

Due to the damaging effect of the inelastically scattered electrons on organic molecules, the images of biological specimens must always be recorded at an exposure not exceeding the critical exposure for each type of specimen in order to obtain high resolution data. As the number of incident electrons is reduced, the signal to noise ratio in the image intensity also decreases, so that only low resolution image features can be detected. For periodic specimens, the signal to noise ratio in the image intensity can be improved upon by spatial averaging of the statistically noisy images of all the unit cells. Using typical

values for the unit cell dimensions, image area, and recorder resolution, we have calculated the possible improvement in the attainable resolution by the SNAP-shot method (section 2.6), and a significant improvement can be expected.

The feasibility of the SNAP-shot method was tested first with a numerical simulation, and then with experimental data taken with an image intensifier. In both cases, we have shown that it is possible to determine the periodicity of an object from its statistically noisy image. When the period of the specimen is known, the statistically determined image can be reconstructed by doing spatial averaging within the computer.

The SNAP-shot method can best be realized with a low-noise detector, which is capable of detecting single electrons, and at the same time has a large area for image data collection. NTB2 emulsion was found to be best suited for this purpose. With an exposure 1000 times less than that required for the Kodak Electron Image Plate, we found that it was possible to obtain an image of high optical density, yet with insignificant fog level.

The grating resolution of the infectiously developed NTB2 emulsion has been determined, and a plot of the attainable resolution vs. magnification indicates that using the SNAP-shot method, it should be possible to obtain 4 Å resolution on NTB2, for a periodic biological specimen with

the typical parameter values chosen in section 5.6.

As indicated previously, better specimen preparation techniques are necessary for the full attainment of high resolution by means of the SNAP-shot method. Better specimen preservation is possible by the use of hydrated specimen techniques, both at room temperature (32), and at liquid nitrogen temperature (44). Electron diffraction patterns of unfixed, unstained, hydrated specimens of catalase crystals showed 2 to 3 Å resolution in both studies cited above, indicating excellent preservation of structure. Specimen hydration can be maintained at room temperature by the use of a differentially pumped hydration stage (32), but at this temperature there probably is considerable brownian motion of the specimen. For this reason, the frozen, hydrated specimen technique is more suitable for the purpose of image recording. Taylor (45) of our laboratory has succeeded in recording images of frozen, hydrated catalase crystals using Kodak No Screen X-ray film. Periodic structure in the images was found out to a resolution of 21 Å. Experiments are currently underway, in our laboratory, to obtain high resolution image data with frozen hydrated specimens, using the SNAP-shot method.

The requirement that the specimen be periodic is not as severe a limitation for structural investigation of biological specimens as it may first seem. Many interest-

ing biological specimens are periodic in the native state. These included the gap junction or nexus, which is a part of the cell surface membrane in many types of tissue (20), the actin and myosin protein found in striated muscle (23), and the gas vacuoles found in bacteria and blue green algae (53). The surface layer of several bacterial species, Spirillum serpens, Micrococcus radiodurans, and several Halobacterium species are composed of periodic arrays of subunits (19,21,40,6). Numerous intracellular inclusions have been reported which occur either as normal storage particles (12) or as pathological fine structure (48), and which exhibit a variety of crystalline or periodic structure. In addition, numerous enzymes and proteins could also be crystallized in vitro to form small crystals suitable for electron microscopic studies.

After the first draft of this thesis was written, we received a pre-print from Unwin and Henderson of the MRC Laboratory of Molecular Biology, at Cambridge, England. They have succeeded in obtaining 7 Å and 9 Å statistically noisy image data of purple membrane and catalase crystals respectively. Glucose was used to facilitate the in vacuo preservation of the specimens, and Kodak Electron Image Plate was used as the image recorder. Their work illustrates beautifully the potential of the SNAP-shot method for high resolution electron microscopy of biological

specimens. Our work differs from theirs in that we make an attempt to optimize the recording process, whereas Unwin aimed at improving the specimen preparation technique and used the conventional Electron Image Plate to demonstrate the improvement in resolution from a well preserved specimen. With the use of NTB2 emulsion which we have found to be a better recording medium, it should be possible to obtain 4 Å resolution of unstained periodic specimens.

APPENDIX

The following are the listings of the main programs and subroutines used for the data analysis in the thesis. The function of the main program and each subroutine is briefly described on the page that immediately precedes the listing.

SNAP....This is the master program. It reads in the various options from data cards, specified by the programmer, and calls the appropriate subroutines to process the input data on a magnetic tape. The various options are listed and explained at the beginning of the program listing. The major subroutines used by the program SNAP to control the sequence of operation are: CUT, FILTER, FOURIER, LOOKPD, LPRINT, SCOPE, TVPICT, TVFOU.

```
      PROGRAM SNAP(INPUT,OUTPUT,TAPE2,
     $TAPE99=101,TAPE3)
C TAPE2 IS THE INPUT TAPE
C TAPE3...MODULUS OF FOURIER ON THIS TAPE. IT IS INPUT TAPE TO PROGRAM
C PICTURE.
C ALLOW MAXIMUM OF 5 PICTURES
C NPICT              NUMBER OF PICTURES(FILES) ON TAPE2
C ITV                SET TO 1 FOR TV DISPLAY
C                    =0,DO NOTHING
C IHEADR             SET TO 1, IF THERE IS A HEADER RECORD IN EACH FILE
C                    =0,DO NOTHING
C ICC                0
C ICUT               1
C IPICT              SET TO 1, FOR 1ST PICTURE
C                    SET TO 2 FOR 2ND PICTURE,ETC.
C IXO,IYO            BEGIN CUT AT IYOTH WORD OF IXOTH RECORD
C LGREY              NUMBER OF GREY LEVEL FOR PICTURE DISPLAY
C IRGEN              SET TO 1, WILL GENERATE RANDOM PATTERN FOR PICTURE
C                    =0,DO NOTHING
C NAVX,NAVY          AVERAGE INPUT DATA BY NAVX COLUMEWISE, AND NAVY
C                    ,ROW-WISE.
C NPEAK              1, WILL LOOK FOR PEAKS IN THE FOURIER SPACE(LEFT)
C                    =0,DO NOTHING
C NUMPK              NUMBER OF PEAKS IN THE LEFT FOURIER SPACE(INCLUDING
C                    ZERO ORDER) TO BE INCLUDED IN THE FILTER
C MINVAL             MINIMUM VALUE OF INPUT DATA
C MAXVAL             MAXIMUM VALUE OF INPUT DATA
C INTVAL             AVERAGED VALUE OF INPUT DATA
C IROW*JCOL          SIZE OF ARRAY TO BE TRANSFORMED
C ISCOPE             =1, WRITE MODULUS OF FOURIER ON TAPE3.
C                    =0, DO NOTHING
C IGSCALE            =1,PLOT GREY SCALE
C                    =0,DO NOTHING
C IDIRT              =1,FOR INPUT DATA LARGER THAN MAXVAL,OR LESSER THAN
C                    MINVAL,SET TO INTVAL
C                    =0,DO NOTHING
C NCOL               NUMBER OF SCANLINE IN A FILE
C MROW               NUMBER OF WORDS IN A SCANLINE.
C IAV                =1,AVERAGE INPUT DATA BY NAVX*NAVY
C                    =0,DO NOTHING
C ISKIPF             NUMBER OF FILES TO BE SKIPPED BEFORE THIS PICTURE.
C                    =0,DO NOTHING
C PNL                EXPONENTIAL POWER FOR IMAGE DISPLAY, NORMALLY=2.
C PNLFOU             EXPONENTIAL POWER FOR FOURIER DISPLAY,NORMALLY=4.
C FOUMAX             CUTOFF FOR FOURIER DISPLAY,ALLOWS 3 VALUES.
      DIMENSION M(3),S(32),INV(32),P(5),TITLE(8),INPUT(1000,5)
      COMPLEX E
      COMMON/BUF/NALL,NALL2,IROWT,NXH,NYH,IERR,NPEAK,TITLE
      COMMON/BUF1/ ROW2, COL2,NALLF
      COMMON/BUF2/ITV,IPR,IAV,IDIRT,IHEADR,IPRIMG,ISHIF
      COMMON/BUF3/MINVAL,MAXVAL,INTVAL
      COMMON E(128,128)
      COMMON/BUF4/IROW,JCOL,LGREY,IRGEN,ISCOPE,IGSCALE,PNL,PNLFOU,
     $PLBL(3),FOUMAX(3)
      COMMON/BUF5/C(3,400)
      COMMON/TVGUIDE/TVMODE,TEXTURE,ITV2
```

```
      LARGE A(131071)
      LARGE AA(73720)
      LARGE B(3,9000)
      DATA PICT/10HPICTURE    /,FOUR/10HFOURIER    /,P/1H1,1H2,1H3,1H4,
     $1H5/,SHIFT/10HSHIFT      /,LATT/10HLATTICE    /
     $,FULL/10HFULL IMAGE/,AUTOFOU/10HAUTOFOU    /
     $,AVIMG/10HAV IMAGE   /
      ITV2=5LDUMMY
      NTAPE=2
      REWIND NTAPE
      REWIND 3
******
      READ 102, TITLE
      PRINT 103,TITLE
******
      READ 100,NPICT,ITV,IHEADR,ICC,ICUT
      IF(ITV .EQ. 1) CALL TVBGN
      IF(ICC .EQ. 1) CALL CCBGN
4     DO 1 I=1,NPICT
******
      READ 102, TITLE
      PRINT 104,TITLE
******
      READ 100,IPICT,IXO,IYO,LGREY,IRGEN,NAVX,NAVY,NPEAK,IPR,ISTAR,
     $ILINEO,NUMPK,MINVAL,MAXVAL,INTVAL
     $,IROW,JCOL,ISCOPE,IGSCALE,IDIRT
******
      READ 100,MROW,NCOL,IAV,ISKIPF
      CALL SKIPFIL(NTAPE,ISKIPF)
      PRINT 112,IPICT
      PRINT 110,MROW,NCOL,IROW,JCOL,IXO,IYO ,NAVX,NAVY,MINVAL,MAXVAL,
     $INTVAL,LGREY
      PRINT 111,ISKIPF,IRGEN,NPEAK,IPR,IAV,ISCOPE,IGSCALE,IDIRT,ISTAR,
     $ILINEO
      IF(NUMPK .EQ. 0) NUMPK=1
******
      READ 107,((B(L,J),L=2,3),J=1,NUMPK)
C POSITION OF PEAKS IN ARRAY B
******
      READ 105,PNL,PNLFOU,FOUMAX
      PRINT 113,PNL,PNLFOU,FOUMAX
      NFRAME=0
      PLBL(2)=P(I)
      PLBL(3)=OB
      NALL=IROW*JCOL
      NALL2=NALL*2
      IROWT=IROW*2
      NYH=IROW/2
      NXH=JCOL/2
      NALLF=IROW*JCOL/4
      ROW2=NXH+1
      COL2=NYH+1
      CALL CUT(A,INPUT,MROW,NCOL,IROW,JCOL,IYO,IXO,NTAPE,NAVX,NAVY,ICUT
      IF(IERR.EQ.2) CALL ERR
      PLBL(1)=PICT
      CALL TVPICT(1,1,128,128,1,1)
```

```
      PNL=1.0
      CALL TVPICT(1,1,128,128,1,1)
      LGREY=32
      CALL TVPICT(1,1,128,128,1,1)
      PNL=2.
      CALL TVPICT(1,1,128,128,1,1)
      CALL FOURIER(320,320,1,-1)
      CALL TVFOU(100,100,128,128,1,1)
      LGREY=16
      CALL TVFOU(100,100,128,128,1,1)
      CALL LPRINT(A,IROW,JCOL,100,100,E,128,128,5,3HMOD     ,1,1,E,IPR,
     $256)
      CALL LPRINT(A,IROW,JCOL,100,100,E,128,128,5,7HCOMPLEX,1,1,E,IPR,
     $256)
      CALL SCOPE(ISCOPE,A,IROW,JCOL,FOUMAX,2,NFRAME,C)
      PRINT 109,NFRAME
      CALL LOOKPO(A,IROW,JCOL,B,IC)
1     CONTINUE
      IF(ITV .EQ. 1) CALL TVEND
      IF(ICC .EQ. 1) CALL CCEND
102   FORMAT(8A10)
103   FORMAT(1H0,8A10)
100   FORMAT(20I4)
104   FORMAT(1H1,8A10)
112   FORMAT(*0PICTURE*,I5,/,13H ************,//,
     $* SPECIFICATION AND OPTIONS*)
110   FORMAT(1H0,10X,*   MROW   NCOL   IROW   JCOL    IXO    IYO   NAVX
     $   NAVY MINVAL MAXVAL INTVAL  LGREY*,/,10X,17I7)
111   FORMAT(1H0,10X,*  ISKIPF  IRGEN  NPEAK    IPR    IAV ISCOPE IGSCA
     $E IDIRT  ISTAR ILINEO*/,10X17I7)
107   FORMAT(20F4.0)
113   FORMAT(1H0, 9X,*        PNL    PNLFOU    FOUMAX*,/,10X,12E10.1)
105   FORMAT(8F10.0)
109   FORMAT(1H0,I9,* FRAME ON SNAPOUT*)
      STOP
      END
```

CUT....Transfers a specified section of the scanned data from the magnetic tape to the large core memory. This subroutine also calls subroutine AVRG which averages the input data.

```
      SUBROUTINE CUT(AR,INPUT,MROW,NCOL,IROW,JCOL,MY,MX,NTAPE,NAVX,NAVY
     $ICUT)
      COMMON/BUF/NALL,NALL2,IROWT,NXH,NYH,IERR,NPEAK,TITLE
      COMMON/BUF1/ ROW2, COL2,NALLF
      COMMON/BUF2/ITV,IPR,IAV,IDIRT,IHEADR,IPRIMG,ISHIF
      COMMON/BUF3/MINVAL,MAXVAL,INTVAL
      DIMENSION INPUT(MROW,NAVX)
      LARGE AR(1)
C
      PRINT 80
80    FORMAT(1H0,*CUT*)
      PRINT 84
84    FORMAT(1H ,3H***)
      IF(ICUT .EQ. 1) GO TO 101
      READ(NTAPE) (AR(I),I=1,NALL2)
      RETURN
101   FNAV=NAVX*NAVY
      IF(MX.LT.1) GOTO 120
      IF(MY.LT.1) GOTO 120
      MX1 = MX-1
      MY2=MY-NAVY+3
      MYE=MY+NAVY*128 + 1
      NCOL1 = NCOL + 1
C IF ARRAY TO BE CUT IS TOO LARGE, RESET DIMENSION
      IF((NCOL-MX-JCOL*NAVX+1) .LT. 0) JCOL=(NCOL-MX+1)/NAVX
      IF((MROW-MY-IROW*NAVY+1).LT. 0) IROW=(MROW-MY+1)/NAVY
      PRINT 83,IROW,JCOL,MY,MX,NAVY,NAVX
83    FORMAT(1H ,*ARRAY DIMENSION...*,I5,* BY*,I5,/,
     $           * CUT BEGIN AT...    *,2I5,/,
     $           * ROW AVERAGED BY...*,I5,/,
     $           * COL AVERAGED BY...*,I5)
C GOTO FIRST LINE REQUESTED
      IF(MX .EQ. 1) GOTO 30
      CALL SKIPREC(NTAPE,MX1,IREC)
      PRINT 82,IREC
82    FORMAT(1H ,*NO. OF RECORDS SKIPPED...*,I5)
      IF(IERR.EQ.2) RETURN
30    CONTINUE
C SKIP HEADER RECORD
      IF(IHEADR .EQ. 1) READ(NTAPE)
C
      DO 50 I=1,JCOL
      DO 40 NZ = 1,NAVX
      READ(NTAPE) (INPUT(K,NZ),K=1,MROW)
      IF(IDIRT .NE. 1) GO TO 40
      DO 60 K=1,MROW
      IN=INPUT(K,NZ)
      IF(IN .GE. MINVAL .AND.
     $   IN .LE. MAXVAL) GO TO 60
      INPUT(K,NZ)=INTVAL
60    CONTINUE
40    CONTINUE
      DO 45 K=1,IROW
      IF(IAV .NE. 1) GO TO 46
      M=((I-1)*IROW+K)*2-1
      AR(M)=AVRG(INPUT(MY2+NAVY*K,1),NAVX,NAVY,MROW)/FNAV
```

```
      AR(M+1)=0.
      GO TO 45
46    K1=K+MY-1
      M=((I-1)*IROW +K)*2-1
47    AR(M)=INPUT(K1,1)
      AR(M+1)=0.
45    CONTINUE
50    CONTINUE
C GO TO EOF
      CALL SKIPREC(NTAPE,NCOL1,IREC)
      PRINT 82,IREC
      IERR=0
100   RETURN
120   IERR=5
      PRINT 81,IERR
81    FORMAT(1X,*IERR=  *,I2)
      END
```

FILTER....Performs the equivalent of an optical filtering on the calculated Fourier transform of the image. This subroutine calls the subroutines AVGPK, ZERO, FILLFOU, LCMFFT, LCMFLIP.

```
      SUBROUTINE FILTER(IAVPK,JAVPK,NUMPK)
      LARGE A(131071),AA(737291),B(3,9000)
      COMMON/BUF/NALL,NALL2,IROWT,NXH,NYH,IERR,NPEAK,TITLE
      COMMON/BUF4/IROW,JCOL,LGREY,IRGEN,ISCOPE,IGSCALE,PNL,PNLFOU,
     $PLBL(3),FOUMAX(3)
      COMMON/BUF5/ C(3,400)
      PRINT 1
1     FORMAT(*0FILTER*,/,7H ******)
      CALL AVGPK(A,IROW,JCOL,B,IAVPK,JAVPK,NUMPK,C)
      CALL ZERO(A,NALL2)
      CALL FILLFOU(C,NUMPK,0.,A,IROW,JCOL )
      CALL LCMFFT(A,IROW,JCOL,1,1)
      CALL LCMFLIP(A,IROW,JCOL)
      RETURN
      END
```

FOURIER....Calls the Fourier transform routine, and converts the transform to a form suitable for display. The subroutines called are LCMFFT, LCMFLIP.

```
      SUBROUTINE FOURIER(IROW,JCOL,N3D,IDIRCT)
      LARGE A(1)
      PRINT 1
      PRINT 2
1     FORMAT(*0FOURIER TRANSFORM*)
2     FORMAT(1H ,17H*****************)
      CALL LCMFFT(A,IROW,JCOL,N3D,IDIRCT)
      CALL LCMFLIP(A,IROW,JCOL)
      RETURN
      END
```

LOOKPD....Finds all the peaks in the diffraction pattern and lists them in a descending order. The subroutines called are HEAPSRT, MAKHEAP, and BUBBLE.

```
      SUBROUTINE LOOKPD(A,IROW,JCOL,B,  IC)
C LOOK FOR PEAKS ONLY IN THE LEFT  HALF   FOURIER SPACE
C DEFINE A PEAK AS AN ELEMENT THAT IS  .GE. ALL ITS NEIGHBOUR
C SEARCH ARRAY A IN COL MAJOR ORDER
C VALUE AND COOR OF PEAKS ARE PRINTED AS THEY ARE ENCOUNTERED IN THE SE
C ONLY ONE PASS IS NECESSARY
C PEAK VALUES STORED IN ARRAY B. THEN B IS SORTED
      LARGE C.A(1)
      LARGE B(3,1)
C NO. OF PEAKS ALLOWED ARE 2000
C FIRST PEAK VALUE A(I,J) STORED IN B(1)
C                         I, STORED IN B(2)
C                         J, STORED IN B(3)
      COMMON/BUF/NALL,NALL2,IROWT,NXH,NYH,IERR,NPEAK,TITLE
      COMMON/BUF1/ ROW2, COL2,NALLF
      COMMON/BUF2/ITV,IPR,IAV,IDIRT,IHEADR,IPRIMG,ISHIF
      COMMON/BUF3/MINVAL,MAXVAL,INTVAL
      IF (NPEAK .EQ. 0) RETURN
      ICOUNT=1
      IROW2=IROW-1
      NXH1=NXH+1
      M=3
      DO 1 J=2,NXH1
      DO 1 I=2,IROW2
       IPK=(J-1)*IROW+I
      AA=CABS(A(IPK))
      IF(AA .GE. CABS(A(IPK-1)) .AND.
     $   AA .GE. CABS(A(IPK+1)) .AND.
     $   AA .GE. CABS(A(IPK+IROW)) .AND.
     $   AA .GE. CABS(A(IPK-IROW)) .AND.
     $   AA .GE. CABS(A(IPK-IROW-1)). .AND.
     $   AA .GE. CABS(A(IPK-IROW+1)) .AND.
     $   AA .GE. CABS(A(IPK+IROW+1)) .AND.
     $   AA .GE. CABS(A(IPK+IROW-1))) GO TO 2
      GO TO 1
C STORE PEAK VALUE IN B(ICOUNT), SUBSCRIPT OF PEAK IN B(ICOUNT+1),B(ICO
2     IF((ICOUNT+2) .GE. NALL) GO TO 3
      B(ICOUNT)=AA
      B(ICOUNT+1)=I
      B(ICOUNT+2)=J
      ICOUNT=ICOUNT+M
      IF(ICOUNT.LE. 27000) GO TO 1
      PRINT 14
      STOP
14    FORMAT(*1 THERE ARE MORE THAN 2000 PEAKS*)
1     CONTINUE
3     IC1=ICOUNT-1
      IC=IC1/M
      PRINT 10,IC
C SORT B. M IS THE NO. OF WORDS IN EACH SORT FRAME
      CALL HEAPSRT(B,IC1,M,IERROR)
      PRINT 12
C REARRANGE B, SUCH THAT LARGEST PEAK IS IN COLUMN 1
      IC2=IC/2
      IC3=IC+1
      DO 5 I=1,IC2
```

```
      IC4=IC3-I
      DO 5 J=1,3
      D=B(J,I)
      B(J,I)=B(J,IC4)
5     B(J,IC4)=D
      IF(IC .GE. 500) IC1=1500
      PRINT 11,(B(I),I=1,IC1)
10    FORMAT(*1NUMBER OF PEAKS FOUND...*,I10)
11    FORMAT(* *,6(1X,E10.2,*(*,F3.0,*,*,F3.0,*)*))
12    FORMAT(*1PEAK VALUES SORTED AS FOLLOWS*)
      RETURN
      END
```

LPRINT....Prints the value of each element of the array which stores the image or the transformed data, to facilitate the plotting of contour lines by hand on the printing paper. It calls GETLCM.

```
      SUBROUTINE LPRINT(A,IROW,JCOL,IB,JB,E,IR,JC,M,MODE,LCMAVX,LCMAVY,
     $CLAR,IPR,IR2)
C PRINT CONTENT OF LCM ARRAY A(IROW,JCOL), STARTING AT(IB,JB),
C PRINT (IR,JC) ELEMENTS OF A, M COL ON ONE PAGE.
C IF MODE=7HCOMPLEX, PRINT REAL AND IMAGINARY PART.
C IF MODE=3HMOD, PRINT MODULUS OF ARRAY A
      LARGE C.A(1)
      DIMENSION CLAR(IR,M),E(IR2,M)
      IF(IPR .NE. 1) RETURN
      PRINT 10
10    FORMAT(6H1*OVF*)
      JN=JB+JC-1
      DO 1 J=JB,JN,M
      CALL GETLCM(A,IROW,JCOL,IB,J,E,IR,M,LCMAVX,LCMAVY)
      IF(MODE.EQ. 7HCOMPLEX) GO TO 2
      IF(MODE .EQ. 3HMOD  ) GO TO 3
3     CALL PACK(E,IR,M)
2     PRINT 11,MODE,J
11    FORMAT(1H1,A10,I10)
12    FORMAT(1H ,I10,5E20.7)
14    FORMAT(1H ,10X,5E20.7)
      DO 4 I=1,IR
      I2=IB+I-1
      IF(MODE.EQ. 7HCOMPLEX) GO TO 5
      PRINT 12,I2,(CLAR(I,JJ),JJ=1,M)
      GO TO 4
5     I3=I*2-1
      I4=I3+1
      PRINT 12,I2,(E(I3,JJ),JJ=1,M)
      PRINT 14,(E(I4,JJ),JJ=1,M)
4     CONTINUE
1     CONTINUE
      PRINT 15
15    FORMAT(6H1*OVN*)
      RETURN
      END
```

SCOPE....Writes the Fourier transformed data onto a magnetic tape, which is used as input to the interactive display program.

```
      SUBROUTINE SCOPE(ISCOPE,A,IROW,JCOL,FOUMAX,IMAX,NFRAME,AVEC)
C WRITES MODULUS OF LCM ARRAY A ONTO TAPE3; ONE COL PER RECORD
      DIMENSION FOUMAX(IMAX),AVEC(1)
      LARGE A(1)
      IF(ISCOPE .NE.1) RETURN
      DO 5 M=1,IMAX
      DO 1 J=1,JCOL
      N=(J-1)*IROW
      DO 2 I=1,IROW
      N1=(N+I)*2
      AVEC(I)=SQRT(A(N1)*A(N1)+A(N1-1)*A(N1-1))
      IF(FOUMAX(1).EQ.0.) GO TO 2
      IF(AVEC(I).GT.FOUMAX(M)) AVEC(I)=FOUMAX(M)
2     CONTINUE
      WRITE(3) (AVEC(L),L=1,IROW)
1     CONTINUE
      END FILE 3
      NFRAME=NFRAME+1
5     CONTINUE
      RETURN
      END
```

TVFOU....Calls a set of subroutines to prepare the Fourier transformed data in a form suitable for Z-modulation display. The subroutines called are GETLCM, PACK, and TVFOU2.

```
      SUBROUTINE TVFOU(IBGN,JBGN,IR,JC,LCMAVX,LCMAVY)
      LARGE A(1)
      COMMON E(256,128)
      COMMON/BUF4/IROW,JCOL,LGREY,IRGEN,ISCOPE,IGSCALE,PNL,PNLFOU,
     $PLBL(3),FOUMAX(3)
      PRINT 1
      PRINT 2
1     FORMAT(*0DISPLAY FOURIER*)
2     FORMAT(16H ***************)
      CALL GETLCM(A,IROW,JCOL,IBGN,JBGN,E,IR,JC,LCMAVX,LCMAVY)
      CALL PACK(E,IR,JC )
      PLBL(1)=7HFOURIER
      CALL TVFOU2(E,IR,JC,PLBL,LGREY,IRGEN,PNLFOU,FOUMAX,2,IGSCALE,0)
      RETURN
      END
```

TVPICT....Prepares the image data for Z-modulation display. The subroutines called are GETLCM, PACK, and TVPICT2.

```
      SUBROUTINE TVPICT(IBGN,JBGN,IR,JC,LCMAVX,LCMAVY)
      LARGE A(1)
      COMMON E(256,128)
      COMMON/BUF4/IROW,JCOL,LGREY,IRGEN,ISCOPE,IGSCALE,PNL,PNLFOU,
     $PLBL(3),FOUMAX(3)
      PLBL(1)=7HPICTURE
      PRINT 1
      PRINT 2
1     FORMAT(*0DISPLAY PICTURE*)
2     FORMAT(16H ***************)
      CALL GETLCM(A,IROW,JCOL,IBGN,JBGN,E,IR,JC,LCMAVX,LCMAVY)
      CALL PACK(E,IR,JC)
      CALL TVPICT2(E,IR,JC,PLBL,LGREY,IRGEN,PNL,0.,IGSCALE)
      RETURN
      END
```

The following subroutines are called by the major subroutines to actually manipulate the data:

AVRG.....averages the input data.

AVGPK....averages the amplitudes and phases of the elements surrounding the selected peaks in the Fourier Transform.

FFT.....this is the fast Fourier transform subroutine, written according to the Singleton algorithm.

FILLFOU..sets the values of the diffraction peaks equal to the averaged values.

LCMFLIP..shifts the calculated Fourier transform, so that the zero order term appears at the center of the array.

GETLCM...retrieves data from any part of the large core memory.

HEAPSRT.
MAKHEAP.
BUBBLE..
} a group of subroutines called by LOOKPD to sort the peaks found in the diffraction pattern.

NORM.....normalizes all elements of an array, such that all values lie between 0 and 1.

PACK.....calculates the modulus of a complex array.

SET.....sets the values in one half of a diffraction pattern according to the Friedel's Law.

SKIPFIL..skips any number of files on the input magnetic tape.

SKIPREC..skips any number of records on a file on the input tape.

TVFOU2...sets the maximum and minimum cutoff values for the display of the diffraction pattern.

TVPICT2..makes a Z-modulation plot of an array; the plot can be displayed on microfilms.

UNPACK...called by subroutine CUT. This converts the input data into a form suitable for Fourier transform.

ZERO.....sets all elements in an array equal to zero.

```
      FUNCTION AVRG(IN,NAVX,NAVY,MROW)
C AVERAGES A NAV*NAV MATRIX
      DIMENSION IN(1)
      LA = 0
      I1 = 0
      DO 30 K = 1,NAVX
      DO 20 I = 1,NAVY
20    LA = LA+IN(I+I1)
      I1 = I1 + MROW
30    CONTINUE
      AVRG = LA
      RETURN
      END
```

```
      SUBROUTINE AVGPK(CLAR,IROW,JCOL,B,KI,KJ,IC,C)
C KI IS THE NO. OF ELEMENTS TO BE AVERAGED IN THE Y-DIRECTION
C KJ IS THE NO. OF ELEMENTS TO BE AVERAGED IN THE X-DIRECTION
C IC IS THE NO. OF PEAKS
C ASSUME THE POSITION OF 1ST PEAK (M,N) IS STORED AT B(2,1),B(3,1)
      DIMENSION C(3,1)
      LARGE CLAR(1)
      LARGE B(3,1)
      COMMON/BUF/NALL,NALL2,IROWT,NXH,NYH,IERR,NPEAK,TITLE
      COMMON/BUF1/ ROW2, COL2,NALLF
      COMMON/BUF2/ITV,IPR,IAV,IDIRT,IHEADR,IPRIMG,ISHIF
      COMMON/BUF3/MINVAL,MAXVAL,INTVAL
      COMMON E(1)
      IK=IC*2-1
      K1=(KI-1)/2
      K2=(KJ-1)/2
      DO 1 I=1,IC
      D1=0.
      D2=0.
C IF PEAK HAS BEEN SET TO (0.,0.) DO NOT DO THE AVERAGING
      M=B(2,I)
      N=B(3,I)
      L1=(N-1)*IROW+M
      L5=2*L1-1
      IF(CLAR(L5) .EQ. 0. .AND. CLAR(L5+1) .EQ. 0.) GO TO 3
      IBGN=M-K1
      JBGN=N-K2
      IEND=IBGN+KI-1
      JEND=JBGN+KJ-1
C CHECK TO SEE IF OFF BOUND. IF SO, DO NOT DO THE AVERAGING FOR THIS PE
      IF(IBGN .LE. 0 .OR.
     $   JBGN .LE. 0 .OR.
     $   IEND .GT. IROW .OR.
     $   JEND .GT.JCOL) GO TO 1
      DO 2 J1=JBGN,JEND
      DO 2 I1=IBGN,IEND
      L2=(J1-1)*IROW+I1
      L3=L2*2-1
      L4=L3+1
      D1=D1+CLAR(L3)
      D2=D2+CLAR(L4)
      CLAR(L3)=0.
2     CLAR(L4)=0.
C SUM OF REAL PART IN C(1,I)
C SUM OF IMAG PART IN C(2,I)
C LINEAR POSITION IN C(3,I)
3     C(1,I)=D1
      C(2,I)=D2
      C(3,I)=L1
      IF(D1 .NE. 0.) GO TO 20
      IF(D2 .GT. 0.) GO TO 21
      E(I)=-1.57
      GO TO 1
21    E(I)=1.57
      GO TO 1
20    E(I)=ATAN(D2/D1)
```

```
1       CONTINUE
        PRINT 11,IK
        PRINT 9,KI,KJ
        PRINT 10,((C(I,J),I=1,2),E(J),(B(K,J),K=2,3),J=1,IC)
        READ 12,((B(K,J),K=2,3),J=1,IC)
12      FORMAT(20F4.0)
        DO 4 I=1,IC
        C(3,I)=(B(3,I)-1.)*IROW+B(2,I)
4       CONTINUE
        PRINT 10,((C(I,J),I=1,2),E(J),(B(K,J),K=2,3),J=1,IC)
9       FORMAT(1H ,I3,* BY*,I3,* AVERAGING OF FOURIER PEAKS*,/,2X,
       $*          REAL        IMAGINARY      PHASE(RAD)    ROW   COL*)
10      FORMAT(3E15.2,2F5.0)
11      FORMAT(*   NUMBER OF PEAKS INCLUDED...*,I5)
        RETURN
        END
```

```
      SUBROUTINE FFT (A,B,NTOT,N,NSPAN,ISN)
C  REFERENCE R.C. SINGLETON,IEEE TRANSACTIONS ON AUDIO & ELECTROACOUSTI
C  AU-17,2,93,JUNE 1969
      LARGE R. A(1),B(1)
      DIMENSION NFAC(11),NP(209)
      DIMENSION AT(23),CK(23),BT(23),SK(23)
      EQUIVALENCE (I,II)
      MAXF=23
      MAXP=209
      IF(N.LT.2) RETURN
      INC=ISN
      RAD=8.*ATANF(1.)
      S72=RAD/5.
      C72=COSF(S72)
      S72=SINF(S72)
      S120=SQRTF(.75)
      IF(ISN.GE.0) GO TO 10
      S72=-S72
      S120=-S120
      RAD=-RAD
      INC=-INC
   10 NT=INC*NTOT
      KS=INC*NSPAN
      KSPAN=KS
      NN=NT-INC
      JC=KS/N
      RADF=RAD*JC*.5
      I=0
      JF=0
      M=0
      K=N
      GO TO 20
   15 M=M+1
      NFAC(M)=4
      K=K/16
   20 IF(K-(K/16)*16.EQ.0) GO TO 15
      J=3
      JJ=9
      GO TO 30
   25 M=M+1
      NFAC(M)=J
      K=K/JJ
30    IF (XMODF(K,JJ).EQ.0) GO TO 25
      J=J+2
      JJ=J**2
      IF(JJ.LE.K) GO TO 30
      IF(K.GT.4) GO TO 40
      KT=M
      NFAC(M+1)=K
      IF(K.NE.1) M=M+1
      GO TO 80
   40 IF(K-(K/4)*4.NE.0) GO TO 50
      M=M+1
      NFAC(M)=2
      K=K/4
   50 KT=M
```

```
      J=2
60    IF (XMODF(K,J).NE.0) GO TO 70
      M=M+1
      NFAC(M)=J
      K=K/J
   70 J=((J+1)/2)*2+1
      IF(J.LE.K) GO TO 60
   80 IF(KT.EQ.0) GO TO 100
      J=KT
   90 M=M+1
      NFAC(M)=NFAC(J)
      J=J-1
      IF(J.NE.0) GO TO 90
  100 SD=RADF/KSPAN
      CD=2.*SINF(SD)**2
      SD=SINF(SD+SD)
      KK=1
      I=I+1
      IF(NFAC(I).NE.2) GO TO 400
      KSPAN=KSPAN/2
      K1=KSPAN+2
  210 K2=KK+KSPAN
      AK=A(K2)
      BK=B(K2)
      A(K2)=A(KK)-AK
      B(K2)=B(KK)-BK
      A(KK)=A(KK)+AK
      B(KK)=B(KK)+BK
      KK=K2+KSPAN
      IF(KK.LE.NN) GO TO 210
      KK=KK-NN
      IF(KK.LE.JC) GO TO 210
      IF(KK.GT.KSPAN) GO TO 800
  220 C1=1.-CD
      S1=SD
  230 K2=KK+KSPAN
      AK=A(KK)-A(K2)
      BK=B(KK)-B(K2)
      A(KK)=A(KK)+A(K2)
      B(KK)=B(KK)+B(K2)
      A(K2)=C1*AK-S1*BK
      B(K2)=S1*AK+C1*BK
      KK=K2+KSPAN
      IF(KK.LT.NT) GO TO 230
      K2=KK-NT
      C1=-C1
      KK=K1-K2
      IF(KK.GT.K2) GO TO 230
      AK=C1-(CD*C1+SD*S1)
      S1=(SD*C1-CD*S1)+S1
      C1=.5/(AK**2+S1**2)+.5
      S1=C1*S1
      C1=C1*AK
      KK=KK+JC
      IF(KK.LT.K2) GO TO 230
      K1=K1+INC+INC
```

```
      KK=(K1-KSPAN)/2+JC
      IF(KK.LE.JC+JC) GO TO 220
      GO TO 100
  320 K1=KK+KSPAN
      K2=K1+KSPAN
      AK=A(KK)
      BK=B(KK)
      AJ=A(K1)+A(K2)
      BJ=B(K1)+B(K2)
      A(KK)=AK+AJ
      B(KK)=BK+BJ
      AK=-.5*AJ+AK
      BK=-.5*BJ+BK
      AJ=(A(K1)-A(K2))*S120
      BJ=(B(K1)-B(K2))*S120
      A(K1)=AK-BJ
      B(K1)=BK+AJ
      A(K2)=AK+BJ
      B(K2)=BK-AJ
      KK=K2+KSPAN
      IF(KK.LT.NN) GO TO 320
      KK=KK-NN
      IF(KK.LE.KSPAN) GO TO 320
      GO TO 700
  400 IF(NFAC(I).NE.4) GO TO 600
      KSPNN=KSPAN
      KSPAN=KSPAN/4
  410 C1=1.
      S1=0.
  420 K1=KK+KSPAN
      K2=K1+KSPAN
      K3=K2+KSPAN
      AKP=A(KK)+A(K2)
      AKM=A(KK)-A(K2)
      AJP=A(K1)+A(K3)
      AJM=A(K1)-A(K3)
      A(KK)=AKP+AJP
      AJP=AKP-AJP
      BKP=B(KK)+B(K2)
      BKM=B(KK)-B(K2)
      BJP=B(K1)+B(K3)
      BJM=B(K1)-B(K3)
      B(KK)=BKP+BJP
      BJP=BKP-BJP
      IF(ISN.LT.0) GO TO 450
      AKP=AKM-BJM
      AKM=AKM+BJM
      BKP=BKM+AJM
      BKM=BKM-AJM
      IF(S1.EQ.0.) GO TO 460
  430 A(K1)=AKP*C1-BKP*S1
      B(K1)=AKP*S1+BKP*C1
      A(K2)=AJP*C2-BJP*S2
      B(K2)=AJP*S2+BJP*C2
      A(K3)=AKM*C3-BKM*S3
      B(K3)=AKM*S3+BKM*C3
```

```
      KK=K3+KSPAN
      IF(KK.LE.NT) GO TO 420
  440 C2=C1-(CD*C1+SD*S1)
      S1=(SD*C1-CD*S1)+S1
      C1=.5/(C2**2+S1**2)+.5
      S1=C1*S1
      C1=C1*C2
      C2=C1**2-S1**2
      S2=2.*C1*S1
      C3=C2*C1-S2*S1
      S3=C2*S1+S2*C1
      KK=KK-NT+JC
      IF(KK.LE.KSPAN) GO TO 420
      KK=KK-KSPAN+INC
      IF(KK.LE.JC) GO TO 410
      IF(KSPAN.EQ.JC) GO TO 800
      GO TO 100
  450 AKP=AKM+BJM
      AKM=AKM-BJM
      BKP=BKM-AJM
      BKM=BKM+AJM
      IF(S1.NE.0.) GO TO 430
  460 A(K1)=AKP
      B(K1)=BKP
      A(K2)=AJP
      B(K2)=BJP
      A(K3)=AKM
      B(K3)=BKM
      KK=K3+KSPAN
      IF(KK.LE.NT) GO TO 420
      GO TO 440
510   C2=.25*SQRTF(5.)
      S2=2.0*C72*S72
  520 K1=KK+KSPAN
      K2=K1+KSPAN
      K3=K2+KSPAN
      K4=K3+KSPAN
      AKP=A(K1)+A(K4)
      AKM=A(K1)-A(K4)
      BKP=B(K1)+B(K4)
      BKM=B(K1)-B(K4)
      AJP=A(K2)+A(K3)
      AJM=A(K2)-A(K3)
      BJP=B(K2)+B(K3)
      BJM=B(K2)-B(K3)
      AK=AKP+AJP
      AJP=(AKP-AJP)*C2
      BK=BKP+BJP
      BJP=(BKP-BJP)*C2
      AKP=A(KK)-0.25*AK
      A(KK)=A(KK)+AK
      BKP=B(KK)-0.25*BK
      B(KK)=B(KK)+BK
      AK=AKP+AJP
      AJP=AKP-AJP
      BK=BKP+BJP
```

```
      BJP=BKP-BJP
      AKP=AKM*S72+AJM*S2
      AKM=AKM*S2-AJM*S72
      BKP=BKM*S72+BJM*S2
      BKM=BKM*S2-BJM*S72
      A(K1)=AK-BKP
      A(K4)=AK+BKP
      B(K1)=BK+AKP
      B(K4)=BK-AKP
      A(K2)=AJP-BKM
      A(K3)=AJP+BKM
      B(K2)=BJP+AKM
      B(K3)=BJP-AKM
      KK=K4+KSPAN
      IF(KK.LT.NN) GO TO 520
      KK=KK-NN
      IF(KK.LE.KSPAN) GO TO 520
      GO TO 700
  600 K=NFAC(I)
      KSPNN=KSPAN
      KSPAN=KSPAN/K
      IF(K.EQ.3)  GO TO 320
      IF(K.EQ.5) GO TO 510
      IF(K.EQ.JF) GO TO 640
      JF=K
      S1=RAD/K
      C1=COSF(S1)
      S1=SINF(S1)
      IF(JF.GT.MAXF) GO TO 998
      CK(JF)=1.
      SK(JF)=0.
      J=1
  630 CK(J)=CK(K)*C1+SK(K)*S1
      SK(J)=CK(K)*S1-SK(K)*C1
      K=K-1
      CK(K)=CK(J)
      SK(K)=-SK(J)
      J=J+1
      IF(J.LT.K) GO TO 630
  640 K1=KK
      K2=KK+KSPNN
      AA=A(KK)
      BB=B(KK)
      AK=AA
      BK=BB
      J=1
      K1=K1+KSPAN
  650 K2=K2-KSPAN
      J=J+1
      AT(J)=A(K1)+A(K2)
      AK=AT(J)+AK
      BT(J)=B(K1)+B(K2)
      BK=BT(J)+BK
      J=J+1
      AT(J)=A(K1)-A(K2)
      BT(J)=B(K1)-B(K2)
```

```
      K1=K1+KSPAN
      IF(K1.LT.K2) GO TO 650
      A(KK)=AK
      B(KK)=BK
      K1=KK
      K2=KK+KSPNN
      J=1
  660 K1=K1+KSPAN
      K2=K2-KSPAN
      JJ=J
      AK=AA
      BK=BB
      AJ=0.
      BJ=0.
      K=1
  670 K=K+1
      AK=AT(K)*CK(JJ)+AK
      BK=BT(K)*CK(JJ)+BK
      K=K+1
      AJ=AT(K)*SK(JJ)+AJ
      BJ=BT(K)*SK(JJ)+BJ
      JJ=JJ+J
      IF(JJ.GT.JF) JJ=JJ-JF
      IF(K.LT.JF) GO TO 670
      K=JF-J
      A(K1)=AK-BJ
      B(K1)=BK+AJ
      A(K2)=AK+BJ
      B(K2)=BK-AJ
      J=J+1
      IF(J.LT.K) GO TO 660
      KK=KK+KSPNN
      IF(KK.LE.NN) GO TO 640
      KK=KK-NN
      IF(KK.LE.KSPAN) GO TO 640
  700 IF(I.EQ.M) GO TO 800
      KK=JC+1
  710 C2=1.-CD
      S1=SD
  720 C1=C2
      S2=S1
      KK=KK+KSPAN
  730 AK=A(KK)
      A(KK)=C2*AK-S2*B(KK)
      B(KK)=S2*AK+C2*B(KK)
      KK=KK+KSPNN
      IF(KK.LE.NT) GO TO 730
      AK=S1*S2
      S2=S1*C2+C1*S2
      C2=C1*C2-AK
      KK=KK-NT+KSPAN
      IF(KK.LE.KSPNN) GO TO 730
      C2=C1-(CD*C1+SD*S1)
      S1=S1+(SD*C1-CD*S1)
      C1=.5/(C2**2+S1**2)+.5
      S1=C1*S1
```

```
      C2=C1*C2
      KK=KK-KSPNN+JC
      IF(KK.LE.KSPAN) GO TO 720
      KK=KK-KSPAN+JC+INC
      IF(KK.LE.JC+JC) GO TO 710
      GO TO 100
  800 NP(1)=KS
      IF(KT.EQ.0) GO TO 890
      K=KT+KT+1
      IF(M.LT.K) K=K-1
      J=1
      NP(K+1)=JC
  810 NP(J+1)=NP(J)/NFAC(J)
      NP(K)=NP(K+1)*NFAC(J)
      J=J+1
      K=K-1
      IF(J.LT.K) GO TO 810
      K3=NP(K+1)
      KSPAN=NP(2)
      KK=JC+1
      K2=KSPAN+1
      J=1
      IF(N.NE.NTOT) GO TO 850
  820 AK=A(KK)
      A(KK)=A(K2)
      A(K2)=AK
      BK=B(KK)
      B(KK)=B(K2)
      B(K2)=BK
      KK=KK+INC
      K2=KSPAN+K2
      IF(K2.LT.KS) GO TO 820
  830 K2=K2-NP(J)
      J=J+1
      K2=NP(J+1)+K2
      IF(K2.GT.NP(J)) GO TO 830
      J=1
  840 IF(KK.LT.K2) GO TO 820
      KK=KK+INC
      K2=KSPAN+K2
      IF(K2.LT.KS) GO TO 840
      IF(KK.LT.KS) GO TO 830
      JC=K3
      GO TO 890
  850 K=KK+JC
  860 AK=A(KK)
      A(KK)=A(K2)
      A(K2)=AK
      BK=B(KK)
      B(KK)=B(K2)
      B(K2)=BK
      KK=KK+INC
      K2=K2+INC
      IF(KK.LT.K) GO TO 860
      KK=KK+KS-JC
      K2=K2+KS-JC
```

```
      IF(KK.LT.NT) GO TO 850
      K2=K2-NT+KSPAN
      KK=KK-NT+JC
      IF(K2.LT.KS) GO TO 850
  870 K2=K2-NP(J)
      J=J+1
      K2=NP(J+1)+K2
      IF(K2.GT.NP(J)) GO TO 870
      J=1
  880 IF(KK.LT.K2) GO TO 850
      KK=KK+JC
      K2=KSPAN+K2
      IF(K2.LT.KS) GO TO 880
      IF(KK.LT.KS) GO TO 870
      JC=K3
  890 IF(2*KT+1.GE.M) RETURN
      KSPNN=NP(KT+1)
      J=M-KT
      NFAC(J+1)=1
  900 NFAC(J)=NFAC(J)*NFAC(J+1)
      J=J-1
      IF(J.NE.KT) GO TO 900
      KT=KT+1
      NN=NFAC(KT)-1
      IF(NN.GT.MAXP) GO TO 998
      JJ=0
      J=0
      GO TO 906
  902 JJ=JJ-K2
      K2=KK
      K=K+1
      KK=NFAC(K)
  904 JJ=KK+JJ
      IF(JJ.GE.K2) GO TO 902
      NP(J)=JJ
  906 K2=NFAC(KT)
      K=KT+1
      KK=NFAC(K)
      J=J+1
      IF(J.LE.NN) GO TO 904
      J=0
      GO TO 914
  910 K=KK
      KK=NP(K)
      NP(K)=-KK
      IF(KK.NE.J) GO TO 910
      K3=KK
  914 J=J+1
      KK=NP(J)
      IF(KK.LT.0) GO TO 914
      IF(KK.NE.J) GO TO 910
      NP(J)=-J
      IF(J.NE.NN) GO TO 914
      MAXF=INC*MAXF
      GO TO 950
  924 J=J-1
```

```
      IF(NP(J).LT.0) GO TO 924
      JJ=JC
  926 KSPAN=JJ
      IF(JJ.GT.MAXF) KSPAN=MAXF
      JJ=JJ-KSPAN
      K=NP(J)
      KK=JC*K+II+JJ
      K1=KK+KSPAN
      K2=0
  928 K2=K2+1
      AT(K2)=A(K1)
      BT(K2)=B(K1)
      K1=K1-INC
      IF(K1.NE.KK) GO TO 928
  932 K1=KK+KSPAN
      K2=K1-JC*(K+NP(K))
      K=-NP(K)
  936 A(K1)=A(K2)
      B(K1)=B(K2)
      K1=K1-INC
      K2=K2-INC
      IF(K1.NE.KK) GO TO 936
      KK=K2
      IF(K.NE.J) GO TO 932
      K1=KK+KSPAN
      K2=0
  940 K2=K2+1
      A(K1)=AT(K2)
      B(K1)=BT(K2)
      K1=K1-INC
      IF(K1.NE.KK) GO TO 940
      IF(JJ.NE.0) GO TO 926
      IF(J.NE.1) GO TO 924
  950 J=K3+1
      NT=NT-KSPNN
      II=NT-INC+1
      IF(NT.GE.0) GO TO 924
      RETURN
  998 ISN=0
      WRITE (6,999)
999   FORMAT(1H1,34H ARRAY BOUNDS EXCEEDED WITHIN FFTS)
      RETURN
      END
```

```
      SUBROUTINE FILLFOU(B,IC,FMIN,A,IROW,JCOL)
C THERE ARE IC PEAKS IN THE COMPLEX ARRAY CLAR
C POSITION OF ITH PEAK IN B(3,I)
C REAL PART OF ITH PEAK IN B(1,I)
C IMAGINARY PART OF ITH PEAK IN B(2,I)
C THIS SUBROUTINE SETS VALUES IN CLAR ACCORDING TO THE POSITION
C SPECIFIES BY B
C FMIN IS THE MIN CUT OFF FOR FILLING FOURIER PEAKS
      COMMON/BUF/NALL,NALL2,IROWT,NXH,NYH,IERR,NPEAK,TITLE
      COMMON/BUF1/ ROW2, COL2,NALLF
      COMMON/BUF2/ITV,IPR,IAV,IDIRT,IHEADR,IPRIMG,ISHIF
      COMMON/BUF3/MINVAL,MAXVAL,INTVAL
      LARGE A(1)
      DIMENSION B(3,IC)
      DO 1 I=1,IC
      J=B(3,I)*2-1
      C=SQRT(B(1,I)*B(1,I)+B(2,I)*B(2,I))
      IF(C .LT. FMIN) GO TO 2
      A(J)=B(1,I)
      A(J+1)=B(2,I)
1     CONTINUE
2      CALL SET(A,IROW,JCOL)
      RETURN
      END
```

```
      SUBROUTINE LCMFLIP(A,IR,JC)
C FLIPS A COMPLEX ARR OF EVEN DIMENSION
      LARGE A(1)
      NH=JC/2
      MH=IR/2
      INCRM=(IR*JC)/2
      DO 1 N=1,NH
      DO 1 M=1,IR
C EXCHANGE A(M,N) AND ITS COUNTER PART
      INDEX=(N-1)*IR+M
      IF(M.GT. MH) GO TO 2
      INDEX2=INDEX+INCRM+MH
      GO TO 3
2     INDEX2=INDEX+INCRM-MH
3     INDEX=INDEX*2-1
      INDEX2=INDEX2*2-1
      TEMP1=A(INDEX)
      TEMP2=A(INDEX+1)
      A(INDEX)=A(INDEX2)
      A(INDEX+1)=A(INDEX2+1)
      A(INDEX2)=TEMP1
      A(INDEX2+1)=TEMP2
1     CONTINUE
      RETURN
      END
```

```
      SUBROUTINE GETLCM(A,IROW,JCOL,IB,JB,E,IR,JC,LCMAVX,LCMAVY)
C CUT A (IR*JC) ARRAY FROM AN ARRAYOF (IROW*JCOL) IN LCM
C AVERAGE ROW BY LCMAVY
C AVERAGE COL BY LCMAVX
C STARTING AT (IB,JB)
      LARGE C.A(1)
      COMPLEX E(IR,JC)
      JB2=JB-1
      IB2=IB-1
      IF((IB2+IR*LCMAVY) .GT. IROW .OR.
     $   (JB2+JC*LCMAVX) .GT. JCOL) GO TO 10
      PRINT 13,IR,JC,LCMAVX,LCMAVY
13    FORMAT(* ARRAY DIMENSION...*,I5,* BY*,I5,/,* AVERAGED...*,I5,* BY
     $*,I5)
      PRINT 12,IB,JB
12    FORMAT(* BEGINS AT LCM LOCATION...*,I4,*,*,I4)
      LCMAVG=LCMAVX*LCMAVY
       N=JB
      DO 1 J=1,JC
      K2=(N-1)*IROW
       M=IB
      DO 4 I=1,IR
C K IS THE LINEAR ADDRESS IN LCM AT WHICH AVERAGING IS TO BEGIN.
      K=K2+M
      E(I,J)=(0.,0.)
C DO AVERAGING
      DO 3 J3=1,LCMAVX
      DO 2 I3=1,LCMAVY
      E(I,J)=E(I,J)+A(K)
2     K=K+1
      K=K+IROW-LCMAVY+1
3     CONTINUE
      E(I,J)=E(I,J)/LCMAVG
      M=M+LCMAVY
4     CONTINUE
      N=N+LCMAVX
1     CONTINUE
      RETURN
10    PRINT 11
11    FORMAT(* GETLCM OUT OF RANGE*)
      RETURN
      END
```

```
      SUBROUTINE MAKHEAP(A,NFAKE,M)
      DIMENSION LARGE(5),TEMP(5)
      LARGE A(1)
      REAL LARGE
      INTEGER TRUVAL
      TRUVAL(K)=M*(K-1)+1
      IF( MOD(NFAKE,2).EQ.0) 10,20
10    IFAKE=NFAKE
      JFAKE=IFAKE/2
      INDEX=IFAKE
      IREAL=TRUVAL(IFAKE)
      DO 101 I1=1,M
         LARGE(I1)= A(IREAL+I1-1)
101   CONTINUE
      GO TO 2
20    IFAKE = NFAKE-1
1     JFAKE=IFAKE/2
      IREAL=TRUVAL(IFAKE)
      DO 102 I2=1,M
         LARGE(I2)=A(IREAL+I2-1)
102   CONTINUE
      INDEX=IFAKE
      IF( A(IREAL).GE. A(IREAL+M)) GO TO 2
      DO 103 I3=1,M
      LARGE(I3)=A(IREAL+M+I3-1)
103   CONTINUE
      INDEX=IFAKE+1
2     JREAL= TRUVAL(JFAKE)
      IF( LARGE(1).LE. A(JREAL))  GO TO 4
      DO 104 I4=1,M
         TEMP(I4)=A(JREAL+I4-1)
         A(JREAL+I4-1)=LARGE(I4)
104   CONTINUE
      CALL BUBBLE(A,NFAKE,M,INDEX,TEMP)
4     IF(IFAKE.EQ.2) RETURN
      IFAKE=IFAKE-2
      GO TO 1
      END
```

```
      SUBROUTINE BUBBLE(A,NFAKE,M,NPOINTR,VAL)
      DIMENSION VAL(M)
      LARGE A(1)
      INTEGER TRUVAL
      TRUVAL(K)=M*(K-1)+1
      INDEX =NPOINTR
5     INDXTRU=TRUVAL(INDEX)
      IF(2*INDEX.GT.NFAKE) GO TO 3
      LSON=2*INDEX
      LSONTRU=TRUVAL(LSON)
      IF(LSON.EQ.NFAKE) GO TO 6
      IF( A(LSONTRU+M).GT. A(LSONTRU) ) LSON=LSON+1
      LSONTRU=TRUVAL(LSON)
6     IF( A(LSONTRU).LE. VAL(1) ) GO TO 3
      DO 10 I1=1,M
         A( INDXTRU+I1-1) = A(LSONTRU+I1-1)
10    CONTINUE
      INDEX=LSON
      GO TO 5
3     DO 11 I2=1,M
         A( INDXTRU+I2-1) = VAL(I2)
11    CONTINUE
      RETURN
      END
```

```
      SUBROUTINE HEAPSRT(A,N,M,IERROR)
      LARGE A(N)
      DIMENSION TEMP(5)
      INTEGER TRUVAL
      TRUVAL(K)=M*(K-1)+1
      IERROR=0
      IF( MOD(N,M).NE.0) GO TO 9000
      NFAKE=N/M
      CALL MAKHEAP(A,NFAKE,M)
1     NREAL=TRUVAL(NFAKE)
      IF( NFAKE.LE.1) RETURN
      DO 2 I=1,M
         TEMP(I)= A(NREAL+I-1)
         A( NREAL+I-1) = A(I)
2     CONTINUE
      NFAKE=NFAKE-1
      CALL BUBBLE(A,NFAKE,M,1, TEMP)
      GO TO 1
9000  IERROR=1
      PRINT 100,N,M
      RETURN
100   FORMAT(//* ***** ERROR *****  *,I7,* IS NOT A MULTIPLE OF *,I5//)
      END
```

```
      SUBROUTINE NORM(A,N,AMIN,AMAX,F,BACKGD)
C CALCULATES MAXIMUM AMAX, MINIMUM AMIN AND NORMALZATION FACTOR F FOR
C THE ARRAY A
C NEED DIFFERENT NORMALIZING PROCEDURE IF BACKGROUND VALUE DIFFER MUCH
C FROM THE IMAGE VALUE.
      COMMON/BUF/NALL,NALL2,IROWT,NXH,NYH,IERR,NPEAK,TITLE
      COMMON/BUF1/ ROW2, COL2,NALLF
      COMMON/BUF2/ITV,IPR,IAV,IDIRT,IHEADR,IPRIMG,ISHIF
      COMMON/BUF3/MINVAL,MAXVAL,INTVAL
      DIMENSION A(N)
      IF( ISHIF .EQ. 1) GO TO 11
      AMIN = A(1)
      AMAX = AMIN
      DO 10 I=1,N
      B=A(I)
      IF(B.LT.AMIN) AMIN=B
      IF(B.GT.AMAX) AMAX=B
10    CONTINUE
      F=1./(AMAX-AMIN)
      RETURN
11    DO 1 I=1,N
      B=A(I)
      IF(B .LE. BACKGD) GO TO 1
      AMIN=B
      AMAX=B
      IBGN=I+1
      GO TO 2
1     CONTINUE
2     DO 3 I=IBGN,N
      B=A(I)
      IF(B .LE. BACKGD) GO TO 3
      IF(B .LT. AMIN) AMIN=B
      IF (B.GT. AMAX) AMAX=B
3     CONTINUE
      F=1./(AMAX-AMIN)
      RETURN
      END
```

```
      SUBROUTINE PACK(CLAR,IR,JC)
C THIS TAKES A COMPLEX IMAGE, PACKS IT INTO A REAL ARRAY.
      COMPLEX CLAR(1)
      COMMON A(1)
      COMMON/BUF/NALL,NALL2,IROWT,NXH,NYH,IERR,NPEAK,TITLE
      COMMON/BUF1/ ROW2, COL2,NALLF
      COMMON/BUF2/ITV,IPR,IAV,IDIRT,IHEADR,IPRIMG,ISHIF
      COMMON/BUF3/MINVAL,MAXVAL,INTVAL
      N=IR*JC
      DO 1 I=1,N
1     A(I)=CABS(CLAR(I))
      RETURN
      END
```

```
      SUBROUTINE SET(A,IROW,JCOL)
C ARRAY A REPRESENTS A COMPLEX FUNCTION F(K). SET THE RIGHT HALF OF F(K
C EQUAL TO THE COMPLEX CONJUGATE OF F(-K)
      COMMON/BUF/NALL,NALL2,IROWT,NXH,NYH,IERR,NPEAK,TITLE
      COMMON/BUF1/ ROW2, COL2,NALLF
      COMMON/BUF2/ITV,IPR,IAV,IDIRT,IHEADR,IPRIMG,ISHIF
      COMMON/BUF3/MINVAL,MAXVAL,INTVAL
      LARGE A(1)
      I1=(NYH+1)*2
      J1=(NXH+1)*2
      JB=NXH+2
      DO 2 J=JB,JCOL
      J2=(J-1)*IROW
      J3=(J1-J-1)*IROW
      DO 2 I=2,IROW
      M=J2+I
      N=J3+I1-I
      M1=2*M-1
      M2=M1+1
      N1=2*N-1
      N2=N1+1
      A(M1)=A(N1)
      A(M2)=-A(N2)
2     CONTINUE
      RETURN
      END
```

```
      SUBROUTINE SKIPFIL(NTAPE,NFILE)
C     THIS WOULD SKIP  NFILE FROM TAPE NTAPE
      IF(NFILE.EQ.0) RETURN
      DO 1 I=1,NFILE
2     READ(NTAPE)
      IF(EOF,NTAPE) 1,2
1     CONTINUE
      RETURN
      END
```

```
      SUBROUTINE SKIPREC(NFILE,NREC,IREC)
C THIS WOULD SKIP NREC NUMBER OF RECORDS FROM THE FILE NFILE.
C IF AN EOF IS ENCOUNTERED , SET IERR=2 AND RETURN
      COMMON /BUF/DUMMY(7),IERR
      IREC=0
      IF(NREC .EQ. 0) RETURN
      DO 1 I=1,NREC
      READ(NFILE)
      IF(EOF,NFILE) 2,3
3     IREC=IREC+1
1     CONTINUE
      RETURN
2     IERR=2
      RETURN
      END
```

```
      SUBROUTINE TVFOU2(AR,IROW,JCOL,PLBL,LGREY,IRGEN,PNL,TVFMAX,IMAX,
     $IGSCALE,ICC)
C CALCULATES A *DIFFRACTOGRAM* , THAT IS, A LOGARITHMIC DISPLAY OF THE
C FOURIER AMPLITUDES OF THE TRANSFORM CLAR.
C THE VALUE AT THE ORIGIN IS SET TO  *ZERO*
C IF ISTAR IS EQ TO 1, SET COL JCOL/2+1 OF FOURIER SPACE =0. THIS IS
C TO ELEMINATE THE INFLUENCE OF THE SCANNER MOTION ON THE TVFOU DISPLAY
C
      COMMON/BUF/NALL,NALL2,IROWT,NXH,NYH,IERR,NPEAK,TITLE
      COMMON/BUF1/ ROW2, COL2,NALLF
      COMMON/BUF2/ITV,IPR,IAV,IDIRT,IHEADR,IPRIMG,ISHIF
      COMMON/BUF3/MINVAL,MAXVAL,INTVAL
      DIMENSION PLBL(3),TVFMAX(3)
      DIMENSION AR(1)
      NT=IROW*JCOL
      IF(TVFMAX(1) .LE. 0.0) RETURN
      DO 2 J=1,IMAX
      DO 10 I=1,NT
      IF(AR(I).GT.TVFMAX(J    )) AR(I)=TVFMAX(J    )
10    CONTINUE
1     CALL TVPICT2(AR,IROW,JCOL,PLBL,LGREY,IRGEN,PNL,0.,IGSCALE)
2     CONTINUE
      RETURN
      END
```

```
      SUBROUTINE TVPICT2(AR,IROW,JCOL,PLBL,LGREY,IRGEN,PNL,BACKGD,
     $IGSCALE)
C MAKES THE INPUT PREPARATION FOR CRT DISPLAY.
C A 1024*1024 CRT FIELD IS DIVIDED INTO 128*128 SUBFIELDS, ONE FOR EACH
C PICTURE ELEMENT. EACH SUBFIELD (J,I) IS FILLED WITH 0...LGREY POINTS
C DISTRIBUTED AT RANDOM, ACCORDING TO THE VALUE OF AR(J,I).
C LGREY IS THE GREY LEVEL DESIRED.HAS MAXIMUM VALUE OF 64 ON CRT
C IRGEN=0, THEN ALL 8*8 RASTOR HAVE SAME RANDOM PATTERN
C IRGEN=1, THEN ALL 8*8 RASTOR HAVE DIFF RANDOM PATTERN
C THE FIRST 4 ROWS OF THE ARRAY AR ARE REPLACED BY A GRAY SCALE.
C INPUT-OUTPUT RELATIONSHIP IS *
C OUTPUT = ((INPUT/LGREY)**PNL)*LGREY
C THIS RELATIONSHIP IS NON-LINEAR IF PNL NE 1.
C AN ARRAY A(IROW,JOCL) CAN BE DISPLAYED WHERE IROW AND JCOL .LE. 128
C
      COMMON/TVTUNE/DUMMY(4),INTENSE,IRIGHT,IUP
      DIMENSION PLBL(1),AR(IROW,JCOL)
      DIMENSION IRX(64),IRY(64)
      COMMON/BUF/NALL,NALL2,IROWT,NXH,NYH,IERR,NPEAK,TITLE
      COMMON/BUF1/ ROW2, COL2,NALLF
      COMMON/BUF2/ITV,IPR,IAV,IDIRT,IHEADR,IPRIMG,ISHIF
      COMMON/BUF3/MINVAL,MAXVAL,INTVAL
      DATA KPTPLOT/50000000B/
      DATA (IRX(I),I=1,16)/5,6,5,4,3,3,3,3,4,5,6,7,8,8,7,6/
      DATA (IRY(I),I=1,16)/5,4,3,2,3,4,5,6,7,7,7,6,5,4,3,2/
      IF(ITV .EQ.0) RETURN
      KORIENT=IRIGHT+INTENSE
      NT=IROW*JCOL
      CALL NORM(AR,NT,AMIN,AMAX,F,BACKGD)
      F1=F *LGREY
C
C DETERMINE COOR OF RANDOM POINTS WITH A 8*8 RASTOR(CORRESPONDING TO 1
C ELEMENT) ON CRT
C THIS PATTERN MAY BE REPEATED OVER THE ENTIRE PICTURE, OR A RANDOM PAT
C GENERATED FOR EACH PICTURE ELEMENT
C
30    CONTINUE
      CALL TVLTR(8., 50.,KORIENT,2,TITLE,80)
      CALL TVLTR(8.,  0.,KORIENT,2,PLBL,30)
      CALL TVNEXT
      DO 100 I=1,JCOL
      IX = 8*I
C GRAYSCALE
C IF IGSCALE .EQ. 1 MEANS A GREY SCALE IS PLOTTED
      IF(IGSCALE .NE. 1) GO TO 40
      IF(I.GT.3) GOTO 40
      DO 38 J = 1,128
      N=(J+1)/(128/LGREY)
      IF(N.EQ.0) GOTO 38
      IF(PNL.EQ.1.) GO TO 39
      RN=N
      N=((RN/LGREY)**PNL)*LGREY
39    JJ=129-J
      IY=8*JJ
      DO 35 K = 1,N
      MX = IX + IRX(K)
```

```
      MY = IY + IRY(K)
      KPLOT = KPTPLOT + 1024*MX + MY
35    CALL TVPACK(KPLOT)
38    CONTINUE
C
      GO TO 100
40    CONTINUE
      DO 100 J=1,IROW
      N =(AR(J,I) - AMIN) * F1 + 0.5
      IF(N .LE. 0) GO TO 100
C PROVISION FOR NONLINEAR INPUT OUTPUT RELATIONSHIP
      IF(PNL.EQ.1.) GO TO 41
      RN=N
      N=((RN/LGREY)**PNL)*LGREY
41    JJ=129-J
      IY=8*JJ
C  PROVISION FOR ALL 8*8 RASTOR TO HAVE DIFF RANDOM PATTERN
      IF(IRGEN .EQ. 0) GOTO 60
      DO 61 L=1,N
      IRX(L)=8.*RGEN(0)
61    IRY(L)=8.*RGEN(0)
60    DO 50 K = 1,N
      MX = IX+IRX(K)
      MY = IY+IRY(K)
      KPLOT = KPTPLOT+1024*MX+MY
50    CALL TVPACK(KPLOT)
100   CONTINUE
      PRINT 120,(PLBL(I),I=1,2),AMIN,AMAX,F,PNL
120   FORMAT(* CRT PREPARATION FOR...*,2A10,
     X*  MIN = *,E15.5,*  MAX = *,E15.5,*  NORMF = *,E15.5/55X,
     $*POWER(NON-LINEAR GREY LEVEL) = *,E15.5)
      CALL TVNEXT
      RETURN
      END
```

```
      SUBROUTINE UNPACK
      LARGE A(1)
      COMMON/BUF/NALL,NALL2,IROWT,NXH,NYH,IERR,NPEAK,TITLE
      COMMON/BUF1/ ROW2, COL2,NALLF
      COMMON/BUF2/ITV,IPR,IAV,IDIRT,IHEADR,IPRIMG,ISHIF
      COMMON/BUF3/MINVAL,MAXVAL,INTVAL
      DO 1 J=1,NALL
      I=(NALL+1)-J
1     A(I*2-1)=A(I)
      DO 2 I=2,NALL2,2
2     A(I)=0.
      RETURN
      END
```

```
      SUBROUTINE ZERO(A,N)
C SETS ALL ELEMENTS IN AN ARRAY OF N ELEMENTS TO ZERO
      LARGE A(1)
      I=0
1     I=I+1
      IF( I.GT. N) RETURN
      A(I)=0.
      GO TO 1
2     RETURN
      END
```

BIBLIOGRAPHY

1. Aebi, U., Smith, P.R., Dubochet, J., Henry, C. and Kellenberger, E., J. Supramolecular Structure, 1, 498 (1974).

2. Bahr, G.F., Johnson, F.B. and Zeitler, E., Lab. Invest. 14, 1115 (1965).

3. Bahr, G.F., Zeitler, E. and Kobayashi, J., J. Appl. Phys., 37, 2900 (1966).

4. Baker, T.T., Photographic Emulsion Technique, 2nd Edition, American Photographic Publishing Co., Boston (1948).

5. Bethe, H.A., Handbook Phys. 24 (1), 273 IV Stosstheorie (1933).

6. Blaurock, A.E. and Stoeckenius, W., Nature New Biology 233, 152 (1971).

7. Charlesby, A., Atomic Radiation and Polymers, Pergamon, Oxford, England (1960).

8. Crowther, R.A., Amos, L.A., Finch, J.T., DeRosier, D.J. and Klug, A., Nature (London) 226, 421 (1970).

9. DeRosier, D.J. and Klug, A., Nature (London) 217, 130 (1968).

10. Dubochet, J., J. of Ultrastruct., 1974, to be published.

11. Erickson, H.P. and Klug, A., Philos. Trans. R. Soc., Lond. Ser. B, Biol. Sci. 261, 105 (1971).

12. Fawcett, D.W., An Atlas of Fine Structure, W.B. Saunders Company (1966).

13. Frank, J., to be published.

14. Frank, J., Bussler, P.H., Langer, R. and Hoppe, W., 7th International Congress on Electron Microscopy, Grenoble, France, 1, 17 (1970).

15. Frank, J., Bussler, P.H., Langer, R. and Hoppe, W., Ber. Bunsenges. Phys. Chem., 74, 1105 (1970).

16. Glaeser, R.M., J. Ultrastruct. Res. 36, 466 (1971).

17. Glaeser, R.M., in Physical Aspects of Electron Microscopy and Microbeam Analysis, B. Siegel ed., John Wiley and Sons (1975).

18. Glauert, A.M., in Techniques for Electron Microscopy, D.H. Kay ed., F.A. Davis Company (1965).

19. Glauert, A.M. and Thornley, M.J., Ann. Rev. Microbiol. 23, 159 (1969).

20. Goodenough, D.A. and Stoeckenius, W., J. Cell Biol. 54, 646 (1972).

21. Holt, S.C. and Leadbetter, E.R., Bacteriol. Rev. 33, 346 (1969).

22. Howitt, D., Master Thesis, University of California, Berkeley (1975).

23. Huxley, H.E. and Brown, W., J. Mol. Biol., 30, 383 (1967).

24. Kobayashi, K. and Sakaoku, K., Lab. Invest. 14, 1097 (1965).

25. Komoda, T., Japan. J. Appl. Phys. 5, 1120 (1966).

26. Kuo, I. and Glaeser, R.M., J. Ultramicroscopy, in preparation.

27. Markham, R., Frey, S. and Hills, G.J., Virology, 20, 80 (1963).

28. Matricardi, V.R., Moretz, R.C. and Parsons, D.F., Science 177, 268 (1972).

29. Matricardi, V., Wray, G. and Parsons, D.F., Micron 3, 576 (1972).

30. Mees, C.E.K. and James, T.H., The Theory of Photographic Process, 3rd Edition (1966).

31. Misell, D.L. and Crick, R.A., Proc. Phys. Soc. London (Solid State Phys.) 2, 2290 (1969).

32. Parsons, D.F., Science 186, 407 (1974).

33. Reimer, L., Lab. Invest. 14, 1082 (1965).

34. Riecke, W.D., Phil. Trans. R. Soc., London, B261, 15 (1971).

35. Rose, A., Adv. Electron, 1, 131 (1948).

36. Salih, S.M. and Cosslett, V.E., Phil. Mag. 30, 225 (1974).

37. Siegel, B.M., Phil. Trans. R. Soc. London, B261, 5 (1971).

38. Siegel, G., Z. Naturforsch. 27a, 325 (1972).

39. Singleton, R.C., IEEE Trans. on Audio and Electroacoustics, AU-17, No. 2, 93 (1969).

40. Sleytr, U.B. and Glauert, A.M., J. of Ultrastruct. Res. 50, 103 (1975).

41. Stauffer, R.E., Smith, W.F. and Trivelli, A.P.H., J. Franklin Inst., 238, 291 (1944).

42. Stenn, K. and Bahr, G.F., J. Ultrastruct. Res. 31, 526 (1970).

43. Stevens, G.W.W., in Fundamental Mechanism of Photographic Sensitivity, London, Butterworth, Scientific Publication, 227 (1951).

44. Taylor, K.A. and Glaeser, R.M., Science 186, 1036 (1974).

45. Taylor, K.A., Ph.D. Thesis, University of California, Berkeley, 1975.

46. Taylor, K.A. and Glaeser, R.M., in preparation.

47. Thach, R.E. and Thach, S.S., Biophys. J. 11, 204 (1971)

48. Thomson, W.W. and Swanson, E.S., 30th Ann. Proc. Electron Microscopic Soc. Amer., 360 (1972).

49. Thon, F., Z. Naturforsh. 20a, 154 (1965).

50. Unwin, P.N.T., Fifth European Congress on Electron Microscopy 232 (1972).

51. Uyeda, N., Kobayashi, T., Suito, E., Harada, Y. and Watanabe, M., 7th Int. Congr. Electron Microsc. Grenoble, (1970).

52. Valentine, R.C. and Wrigley, N.G., Nature 203, 713 (1964).

53. Walsby, A.E., Bacteriological Reviews, 36, 1 (1972).

54. Wrigley, N.G., J. Ultrastruct. Res. 24, 454 (1968).

55. Williams, R.C. and Fisher, H.W., J. Mol. Biol., 52, 121 (1970).

56. Yada, K. and Hibi, T., J. Electronmicrosc. 18, 266 (1969).

57. Zeitler, E. and Thompson, M.G.R., Optik 31, 258 (1970).

ACKNOWLEDGMENTS

I would like to express my deepest gratitude to Professor Robert Glaeser who has provided valuable guidance and advice throughout my graduate studies. I would also like to thank Professors Robley Williams and Alexander Nichols for their reading of this thesis and for their many valuable suggestions. In addition, I thank Paul Banchero, Don Austin, Victor Elisher, Jim Nichols, Paul Ridder and David Grano who have provided assistance in various aspects of the project.

This work has been supported in part by USPHS Training Grant No. 5 T01 GM00829 from the National Institute of General Medical Sciences.

LEGAL NOTICE

This report was prepared as an account of work sponsored by the United States Government. Neither the United States nor the United States Energy Research and Development Administration, nor any of their employees, nor any of their contractors, subcontractors, or their employees, makes any warranty, express or implied, or assumes any legal liability or responsibility for the accuracy, completeness or usefulness of any information, apparatus, product or process disclosed, or represents that its use would not infringe privately owned rights.

TECHNICAL INFORMATION DIVISION
LAWRENCE BERKELEY LABORATORY
UNIVERSITY OF CALIFORNIA
BERKELEY, CALIFORNIA 94720